Journal Pre-proof

IL-1β-primed Mesenchymal Stromal Cells improve epidermal substitute engraftment and wound healing via MMPs and TGF-β1

B. Magne, M. Dedier, M. Nivet, B. Coulomb, S. Banzet, J.J. Lataillade, M. Trouillas

PII: S0022-202X(19)33214-2

DOI: https://doi.org/10.1016/j.jid.2019.07.721

Reference: JID 2138

To appear in: *The Journal of Investigative Dermatology*

Received Date: 12 April 2019

Revised Date: 18 July 2019

Accepted Date: 31 July 2019

Please cite this article as: Magne B, Dedier M, Nivet M, Coulomb B, Banzet S, Lataillade JJ, Trouillas M, IL-1β-primed Mesenchymal Stromal Cells improve epidermal substitute engraftment and wound healing via MMPs and TGF-β1, *The Journal of Investigative Dermatology* (2019), doi: https://doi.org/10.1016/j.jid.2019.07.721.

This is a PDF file of an article that has undergone enhancements after acceptance, such as the addition of a cover page and metadata, and formatting for readability, but it is not yet the definitive version of record. This version will undergo additional copyediting, typesetting and review before it is published in its final form, but we are providing this version to give early visibility of the article. Please note that, during the production process, errors may be discovered which could affect the content, and all legal disclaimers that apply to the journal pertain.

© 2019 The Authors. Published by Elsevier, Inc. on behalf of the Society for Investigative Dermatology.

Journal Pre-proof

IL-1β-primed Mesenchymal Stromal Cells improve epidermal substitute engraftment and wound healing via MMPs and TGF-β1

Running head of the title:

IL-1β-primed MSC favor wound healing

B. Magne[1,2,3], M. Dedier[1], M. Nivet[1,2], B. Coulomb[2,3], S. Banzet[1,2], J.J. Lataillade[1,2], M. Trouillas[1,2]

[1]IRBA (French Armed-forces Biomedical Research Institute), Clamart, France

[2]INSERM UMR-1197, Villejuif, France

[3]Scarcell Therapeutics, Paris, France

Journal Pre-proof

Journal Pre-proof

Corresponding author

Marina Trouillas, PhD

Unité mixte Inserm UMR-1197 - Institut de Recherche Biomédicale des Armées (IRBA)

Antenne Centre de Transfusion Sanguine des Armées

1 rue du Lieutenant Raoul BATANY

BP 410

92141 CLAMART cedex

Email : marina-laurie.trouillas@inserm.fr

Tel : + 33.1.41.46.72.09

Fax : + 33.1.41.46.72.81

Journal Pre-proof

Journal Pre-proof

ABSTRACT

Since the 1980s, deep and extensive skin wounds and burns are treated with autologous Split-Thickness Skin Grafts, or Cultured Epidermal Autografts (CEAs) when donor sites are limited. However, the clinical use of CEAs often remains unsatisfactory due to poor engraftment rates, altered wound healing and reduced skin functionality.

In the past few decades, Mesenchymal Stromal Cells (MSCs) have raised much attention due to their anti-inflammatory, pro-trophic and pro-remodeling capacities. More specifically, gingival MSCs have been shown to possess enhanced wound healing properties compared to other tissue sources. Growing pieces of evidence have also indicated that MSC priming could potentiate therapeutic effects in diverse *in vitro* and *in vivo* models of skin trauma.

In the present study, we found that, IL-1β-primed gingival MSCs (IL-MSCs) promoted cell migration, dermal-epidermal junction formation and inflammation reduction *in vitro*, as well as improved epidermal substitute engraftment *in vivo*. IL-MSCs had different secretory profiles from naive gingival MSCs (NV-MSCs), characterized by an overexpression of TGF-β and MMP pathway agonists. Eventually, MMP-1, MMP-9 and TGF-β1 appeared to be critically involved in IL-MSC mechanisms of action.

Journal Pre-proof

KEYWORDS

Mesenchymal stromal cells

Preconditioning / Priming

Wound healing

Severe burn

Skin graft

LIST OF ABBREVIATIONS

CM: Conditioned Medium

CEA: Cultured Epidermal Autograft

hPBES: human Plasma-based Epidermal Substitute

IL-CM: IL-1β primed MSC Conditioned Medium

NV-CM: naive MSC Conditioned Medium

COL-4: Collagen-4

CK-10: Cytokeratin-10

DEJ: Dermal-Epidermal Junction

ECM: Extracellular Matrix

IL-1β: Interleukin-1β

LAM-5: Laminin-5

LAM-γ2 : Laminin-5 gamma-2-chain

Journal Pre-proof

MSC: Mesenchymal Stromal Cell

IL-MSC: IL-1β-primed MSC

NV-MSC: naive MSC

NID-1: Nidogen-1

TNC: Tenascin-C

Journal Pre-proof

Journal Pre-proof

INTRODUCTION

Skin is essential to protect the body against infections and water loss. Upon injury, immune and skin cells trigger a cascade of events to orchestrate the wound repair. However, in case of full-thickness injuries or massive burns, this process is delayed. The current gold standard uses skin autografts, but is limited by donor site availability. Alternative therapies combine surgery and Cultured Epidermal Autografts (CEAs) or keratinocytes in spray (Chua et al., 2016, Ter Horst et al., 2018), but remain unsatisfactory due to persistent inflammation, poor skin engraftment and immature Dermal-Epidermal Junction (DEJ) (Auxenfans et al., 2015, Cirodde et al., 2011).

Mesenchymal Stromal Cells (MSCs) have become an attractive therapeutic option to improve tissue repair and treat severe skin disorders in clinical cases (Cerqueira et al., 2013, Gaur et al., 2015). Preclinical studies have highlighted their potential to reduce inflammation and promote reepithelialization and extracellular matrix (ECM) remodeling through paracrine mechanisms (Chen et al., 2016, Jackson et al., 2012). However, MSCs isolated from different tissue sources may not possess the same healing properties (Macrin et al., 2017). The gingiva is a tissue that heals fast with mild inflammation and minimal scar formation (Glim et al., 2013). Due to its location, it remains well-preserved from traumatic injuries, and easily accessible for cell harvest. From a clinical perspective, gingival tissues yield more proliferative (Li et al., 2018, Tomar et al., 2010) and clonogenic cells than the bone marrow (Fournier et al., 2010). At last, healing properties of gingival cells are seemingly superior to those of bone marrow MSCs to treat radiation burns (Linard et al., 2015).

MSCs are known to sense their environment and adapt accordingly (Kusuma et al., 2017). Using specific priming cues, such as cytokines, it is possible to guide MSC (Madrigal et al., 2014). However, to reach therapeutic outcomes, MSC priming must be carefully chosen depending on the disorder to treat (Magne et al., 2018). In the context of skin wound healing,

Journal Pre-proof

inflammatory primings have been reported to substantially improve MSC therapies (Heo et al., 2011).

Interleukin-1β (IL-1β) is released early after injury and can persist at high levels long after severe skin traumas, such as burns (Jeschke et al., 2008). In the gingival tissue, this cytokine is known to promote the secretion of matrix metalloproteinases (MMPs), chemokines and prostaglandins (Preshaw and Taylor, 2011), that contribute to the process of wound healing (Singer and Clark, 1999). Recent studies have shown that IL-1β-primed non-gingival MSCs could reduce inflammation (Fan et al., 2012, Song et al., 2017) and stimulate wound closure *in vivo* (Park et al., 2018). However, no study has yet addressed the effect of IL-1β-primed gingival MSCs (IL-MSCs) on skin wound healing and epidermal graft take after major skin injuries.

In the present study, we therefore investigated whether IL-MSCs were superior to naive MSCs (NV-MSCs) to improve wound healing and epidermal engraftment *in vitro* and *in vivo*. Our results demonstrated that IL-MSCs reduced inflammation, stimulated migration and DEJ formation and promoted epidermal engraftment, through the secretion of MMPs and TGF-β1. Taken together these results open up exciting avenues for future clinical applications.

Journal Pre-proof

RESULTS

IL-1β-primed MSCs support wound healing and epidermal maturation *in vitro*

MSCs isolated from gingival tissues were plastic adherent, able to differentiate into osteogenic, adipogenic and chondrogenic lineages, and expressed characteristic markers (Figure S1). We investigated the impact of naive and IL-1β-primed gingival MSCs (NV- and IL-MSCs) on skin wound healing *in vitro*. We first developed a wound closure assay in which we intoxicated keratinocytes with a cocktail of stress molecules known to be overexpressed during traumatic skin injuries (D'Arpa and Leung, 2017, Stanojcic et al., 2018) (see "Material & Method"). IL-MSCs strongly accelerated the wound closure of intoxicated keratinocytes ($p < 0.05$) and faster than NV-MSCs ($p < 0.05$, Figure 1a). Using an air/liquid differentiation assay, we then showed that IL-MSCs slightly increased epidermal thickness ($p = 0.11$), significantly supported basal layer organization ($p < 0.05$, Figure 1b), and promoted Cytokeratin-10 (CK-10, Figure 1c) expression compared to control or NV-MSCs in a human Plasma-Based Epidermal Substitute (hPBES, a CEA developed in our laboratory (Alexaline et al., 2015). Both NV- and IL-MSCs promoted the deposition of DEJ proteins including Tenascin-C (TNC), Laminin-5 (LAM-5) and Collagen-4 (COL-4) (Figure 1c). At last, NV-MSC and IL-MSCs drastically reduced the inflammatory response of a LPS-challenged monocytic THP1cell line, as depicted by a high increase of IL-1RA ($p < 0.01$, Figure 1d) and a strong decrease of TNF-α ($p < 0.01$, Figure 1e) in THP-1 culture supernatants. Interestingly, IL-MSCs were superior to NV-MSCs to decrease TNF-α secretions ($p < 0.05$, Figure 1e). Taken together, these results suggest that IL-MSCs are superior to NV-MSCs to promote wound closure, hPBES maturation and decrease of inflammation.

IL-1β-primed MSCs support hPBES engraftment and wound healing *in vivo*

We next compared the wound healing potential of NV- and IL-MSCs in a NOD/SCID mouse

Journal Pre-proof

model of full-thickness injury and hPBES grafting. Based on preliminary dose-effect studies, treated mice received 750,000 MSCs (Figure S2). Our results indicated that IL-MSCs strikingly increased the engraftment rate of hPBES compared to the control ($p < 0.05$, Figure 2a). While NV- and IL-MSCs did not improve the basal cell organization of grafted hPBES (p = ns), IL-MSCs significantly favored the epidermal thickness compared to control ($p < 0.05$) and tended to have a more prominent effect than NV-MSCs ($p = 0.16$, Figure 2b). NV- and IL-MSCs also improved the expression of epidermal differentiation marker CK-10, and DEJ proteins such as TNC, LAM-5 and COL-4 in grafted hPBES (Figure 2c). Lastly, we noted that IL-MSCs induced a shift towards a M2-polarization with a significant drop of $iNOS^+/CD206^+$ cell ratio compared to the control ($p < 0.01$), while NV-MSCs did not (p = ns, Figure 2c-d). To conclude, while NV- and IL-MSCs seemed to have similar effects on hPBES maturation and DEJ deposition, IL-MSCs were more efficient to support hPBES engraftment and thickening *in vivo*.

MSC secretome is significantly modified by IL-1β priming

As IL-MSCs appeared to possess superior repair properties *in vitro* and *in vivo*, we next sought to decipher their mechanisms of action. Therefore, we investigated how IL-1β priming could modify MSC secretome, since these cells mainly operate through paracrine mechanisms (Gnecchi et al., 2016). Mass spectrometry analysis of naive and IL-1β-primed MSC Conditioned Media (NV-CM and IL-CM respectively) revealed substantial differences in terms of protein content and expression level (Figure 3a, Table S1). We noted that the IL-1β priming induced the expression of 76 proteins uniquely found in IL-CM. Based on protein intensity scores, a higher expression of proteins related to migration, angiogenesis, remodeling, inflammation, SMAD, Integrin and Wnt pathways was found in IL-CM compared to NV-CM (Figure 3b). These data were supported by a protein interaction study using the online "String" data base (Figure S3a). To confirm these results, we quantified by

Journal Pre-proof

ELISA a selection of wound healing-related proteins and found that active MMP-1, active MMP-9, HGF, IGFBP-7, STC-1, TGF-β1 (Figure 3c), VEGF, FGF-2, FGF-7, IL-6, IL-1RA and SOD-2 (Figure S3b) were up-regulated in IL-CM compared to NV-CM ($p < 0.05$). Taken together, these findings reveal that MSCs secrete higher levels of wound healing-related factors after IL-1β priming.

Beneficial effects of IL-1β-primed MSCs relies on distinct paracrine secretions

Given the differences between NV- and IL-CM, we next sought to investigate their effect *in vitro*. Our findings revealed that IL-CM had a higher pro-migratory effect than NV-CM on intoxicated keratinocytes ($p < 0.05$, Figure 4a). IL-CM also tended to improve the expression level of several DEJ proteins, including Nidogen-1 (NID-1) ($p = 0.094$), TNC (p = ns) and Laminin-5 gamma-2 chain (LAM-γ2) ($p = 0.094$) compared to control (Figure 4b-d). Lastly, IL-CM presented stronger anti-inflammatory properties than NV-CM, as shown by the significant drop of TNF-α ($p < 0.001$, Figure 4e) and increase of IL-1RA ($p < 0.001$, Figure 4f) in LPS-challenged THP-1 supernatants. Importantly, THP-1 were the main producers of TNF-α and IL-1RA, as these factors were respectively absent (data not shown) or barely expressed in IL-CM (Figure S4a). Taken together, these data imply that IL-MSCs secrete distinctive factors that better regulate the skin wound healing than those derived from NV-MSCs.

MMPs and TGF-β1 are key mediators involved in the mechanism of action of IL-1β-primed MSCs

Rapid and scarless gingival repair is thought to rely on superior remodeling and anti-inflammatory properties of gingival cells (Leavitt et al., 2016, Mah et al., 2017). According to our secretome analysis (Figure 3b-c), we therefore focused on MMPs and SMAD signaling to investigate the mechanisms of action of IL-CM. We used Tigecycline, a broad-spectrum

Journal Pre-proof

inhibitor of MMPs (Pasternak and Aspenberg, 2009), SB431542, an inhibitor of the TGF-β receptor 1 (Inman et al., 2002), and human recombinant MMP-1, MMP-9, TGF-β1, HGF, IGFBP-7, STC-1 and QSOX-1 (used alone or combined in a cocktail, at the concentration they were found in IL-CM by ELISA). We showed that Tigecycline clearly prevented the IL-CM-induced migration of intoxicated keratinocytes ($p < 0.01$), while SB431542 did not (p = ns, Figure 5a). These results were confirmed using MMP-1 which significantly increased intoxicated keratinocytes migration ($p < 0.01$), while TGF-β1 or any other protein tested did not (p = ns, Figure 5b and S4b). Regarding DEJ protein expression, SB431542 abrogated the effect of IL-CM on NID-1 ($p<0.05$, Figure 5c) and tended to suppress the expression of TNC and LAM-γ2 (Figure 5d-e). Tigecycline abolished the effect of IL-CM on NID-1 only ($p < 0.05$, Figure 5c). When used alone in control experiments, both inhibitors did not induce DEJ protein expression drop, except for NID-1 with Tigecycline ($p=0.086$, Figure S5). We next observed that MMP-1, MMP-9 and TGF-β1 could possibly improve NID-1 (p = ns, Figure 5f and S4c) and TNC expression (p = ns, Figure 5g and S4d). However, none of the tested proteins increased LAM-γ2 expression (Figure 5h and S4e). At last, none of the tested inhibitors (Figure 5i), or tested proteins were able to block the effect of IL-CM on TNF-α production in LPS-challenged THP-1 supernatants (p = ns, Figure 5j and S4f). Conversely, both inhibitors abrogated the effect of IL-CM on IL-1RA ($p < 0.05$ and $p < 0.01$ respectively, Figure 5k). Recombinant TGF-β1 ($p < 0.01$), MMP-9 ($p < 0.05$), HGF ($p < 0.01$), IGFBP-7 ($p < 0.05$) and the protein cocktail ($p < 0.01$) significantly increased the expression of IL-1RA (Figure 5l and S4g). Taken together, these results suggest that IL-MSCs promote migration, DEJ protein deposition and reduction of inflammation through the synthesis of MMPs and TGF-β1.

Journal Pre-proof

DISCUSSION

In an attempt to improve the clinical management of full-thickness injuries and burns, we aimed to bring forward MSC therapy using a specific tissue source and an inflammatory priming. IL-1β is known to play important roles in oral mucosal wound healing (Graves et al., 2001), but is also a key pathological mediator in inflammatory oral diseases. In this study, the priming dose was below the levels observed in patients with gingivitis or periodontitis (Orozco et al., 2006). Therefore, we showed that IL-MSCs promoted skin wound closure, DEJ protein deposition, reduction of inflammation and, epidermal engraftment through a paracrine mechanism involving MMPs and TGF-β1 signaling (Figure 6).

As many other investigators, we found that the IL-1β priming of MSCs led to major secretome changes in terms of growth factors, inflammatory mediators and ECM components (Figure 3 and S3) (Lee et al., 2010, Maffioli et al., 2017, Redondo-Castro et al., 2018). Up-regulated growth factors such as FGF-2, FGF-7, HGF and TGF-β1 may have helped promote the keratinocyte migration (Peplow and Chatterjee, 2013, Seeger and Paller, 2015), although we did not see a beneficial effect of individual factors (Figures 5b and S4b). As shown in our study, and in line with previous works (Benjamin and Khalil, 2012), MMP1 also clearly contributed to the promotion of keratinocyte migration (Figure 5b). Enhanced secretion of TGF-β1, MMP-9, HGF and IGFBP-7 following the IL-1β priming increased the release of IL-1RA by LPS-challenged THP-1 cells (Figure 5l and S4g), highlighting their anti-inflammatory role, as previously reported (de Araujo Farias et al., 2018). Our results investigating the mechanism of IL-CM on decreasing secretion of TNF-α also suggest that other paracrine factors might be involved, such as TSG-6 (Qi et al., 2014). The overexpression of TGF-β1 and MMPs in IL-CM was shown to have an overall positive impact on the production of DEJ proteins, although this effect was not always obvious *in vitro* (Figure 5f-h and S4c-e). Such inconsistencies are probably due to the dual role of MMPs that

Journal Pre-proof

degrade DEJ proteins like COL-4 (Monaco et al., 2006) and activate DEJ-stimulating growth factors like TGF-β1 (Benjamin and Khalil, 2012). However, our results indicate that enhanced DEJ protein deposition and decreased inflammation *in vivo* might have contributed to the promotion of epidermal engraftment and maturation (Figure 2 and S2). Indeed, other studies have reported a better epidermal engraftment when DEJ proteins were preserved or added exogenously (Alexaline et al., 2019, Takeda et al., 1999). Recent studies have also shown that MSCs contribute to DEJ restoration through direct secretion of type VII collagen (Ganier et al., 2018) or exosomes containing both protein and mRNA (McBride et al., 2018). In our secretome analysis, increased expression levels of type IV and VII collagens, and nidogens were found in IL-CM, confirming previous results showing that IL-1β primed skin cells secrete basement membrane protein in higher amount (Furuyama et al., 2008, Matsushima et al., 1985, Mauviel et al., 1994, Vardar-Sengul et al., 2009). Therefore, the beneficial effect of IL-1β primed MSC must be due to a combination of direct DEJ protein deposition or an indirect stimulation of DEJ-producing resident cells, such as keratinocytes and fibroblasts.

In our study, we focused on MMPs and TGF-β signalings to unravel the mechanism of action of IL-MSCs. However, several other molecular pathways may be worth explore such as the MAPK, Akt, Integrin and Wnt/β-catenin (Longmate and Dipersio, 2014, Park et al., 2018). Importantly, previous works have shown that IL-1β could activate the Wnt/β-catenin pathway, resulting in more angiogenesis (Sun et al., 2016) and increased production of MMPs (Ge et al., 2009). This signaling pathway was also shown to promote cell migration in a model of burn wound through the release of Wnt4-carrying exosomes (Zhang et al., 2014, Zhang et al., 2015).

In conclusion, IL-1β-primed MSCs represent a promising therapeutic option for future cell-based therapy of full-thickness injuries, improving wound healing and epidermal substitute engraftment. Although our study focused on whole CM, we found that most of

Journal Pre-proof

them were composed of extracellular vesicles (data not shown). It is thus possible that the reported effects of IL-1β primed MSCs are accountable for the presence of extracellular vesicles carrying growth factors, cytokines or extracellular components. Therefore, the present study highlights the therapeutic benefit of using MSC secretory products to improve the treatment of severe skin traumas.

MATERIALS AND METHODS

Cell isolation, culture and characterization

After written informed patient consent, gingival MSCs, skin fibroblasts and keratinocytes were extracted from human donor biopsies (Supplemental Materials and Methods) and cultivated in medium, as described previously (Alexaline et al., 2015, Doucet et al., 2005). The human THP1 cell line (ATCC) was cultured in RPMI medium supplemented with 10 % decomplemented FCS, 50 µM β-mercapto-ethanol (Sigma) and penicillin-steptomycin (100 U/mL, 100 µg/mL respectively, Gibco). Gingival MSCs were characterized by flow cytometry and differentiation assays (Supplemental Materials and Methods).

MSC Priming and Conditioned Medium (CM) preparation

Passage 4 MSCs were cultivated until 60% confluence, primed for 24h with 1 ng/ml human recombinant IL-1β (Peprotech) or left naive with no treatment. The priming dose was selected according to preliminary studies (data not shown). IL-MSCs or NV-MSCs were then washed three times in PBS and incubated in serum- and antibiotic-free medium for 48h. NV-CM and IL-CM were respectively derived from NV-MSC and IL-MSC supernatants and concentrated 40X using Amicon ultra centrifugal filter units (cutoffs 3K, Millipore) (Figure S6a). CM total protein amount was determined using the Bio-Rad Protein Assay kit. CM were analyzed using mass spectrometry and ELISA (Supplemental Materials and Methods).

Journal Pre-proof

Wound closure Assay

31,500 irradiated (60 grays of γ rays) passage 1 keratinocytes were seeded in each well of migration silicone inserts (Ibidi) with complete KSFM medium (Gibco). After insert removal, keratinocytes were washed with PBS and new medium was added along with an intoxication cocktail (1.31 mg/ml NaCl (Sigma), 0.23 mg/ml $NaHCO_3$ (Sigma), 1 ng/mL IL-1β (Peprotech), 1 ng/mL IL-6 (Peprotech) and 10 ng/mL HMGB1 (Peprotech)), optimized in preliminary studies (data not shown). Keratinocytes were co-cultured with a pool of NV-MSCs or IL-MSCs from 7 donors at a 1:10 MSC-to-keratinocyte ratio in 0.4µm pore culture inserts (PET membrane, EMD-Millipore), a pool of NV-CM or IL-CM from 7 donors at 10µg/mL, SB431542 at 10µM (all from Calbiochem), Tigecycline at 50µM (Pfizer), or specific recombinant human factors including MMP-1 at 35.3 pg/ml, MMP-9 at 33.8 pg/ml, TGF-β1 at 5 ng/ml, STC-1 at 350 pg/ml, HGF at 50 pg/ml, IGFBP-7 at 5 ng/ml or QSOX-1 at 350 pg/ml (all from R&D) (Figure S6b). The cocktail includes TGF-β1, MMP-1, MMP-9, STC-1, HGF, QSOX-1 and IGFBP-7. Pictures of the entire gap were taken at 5 hours, and analyzed using the Image J software (1.47v). Wound closure percentage was calculated: 100 x $(A_{T0}-A_{T5H})/A_{T0}$, with A_{T0}: Area of the gap at 0H, A_{T5H}: Area of the gap at 5H.

DEJ Formation Assay

Passage 1 keratinocytes were seeded and cultured on a confluent irradiated fibroblast feeder layer (Supplemental Materials and Methods). At day 4 and day 6, culture medium was supplemented with a pool of NV-CM or IL-CM from 7 donors at 10µg/mL, inhibitors or specific recombinant human growth factors (see "Wound closure assay" section) (Figure S6c). At day 8, keratinocytes were washed with PBS and lysed for further analysis of LAM-γ2, NID-1 and TNC expression by Western Blot (Supplemental Materials and Methods).

Air/liquid differentiation assay

hPBES were prepared as described previously ((Alexaline et al., 2015), Supplemental Materials and Methods) and transferred in 0.4 µm pore 6-well culture inserts (PET membrane, EMD Millipore), previously seeded with a pool of 25,000 NV-MSCs or IL-MSCs from 7 donors, and were grown in keratinocyte culture medium at the air/liquid interface for 7 days, with medium change every 2 to 3 days (Figure S6d). At day 7, hPBES were fixed, embedded in paraffin and processed for Hematoxylin-Phloxin-Safranin (HPS) staining and CK-10, COL-4, LAM-5 and TNC immunostainings (Supplemental Materials and Methods). Basal epidermal organization was scored as described elsewhere (Figure S7).

Inflammation Assay

THP1 cells were seeded in 24-well plates at 170,000 cells/mL, exposed to 1 µg/mL LPS (Escherichia coli O55:B5; Sigma) and cultured with a pool of NV-MSCs or IL-MSCs from 7 donors at a 1:10 MSC-to-THP1 ratio, a pool of NV-CM or IL-CM from 7 donors at 10µg/mL, inhibitors or specific human recombinant growth factors (see "Wound closure assay" section) (Figure S6e). Supernatant of each condition was collected after 24h and assayed for TNF-α and IL-1RA levels by ELISA (DuoSet® Kits, R&D Systems).

Animal model of dorsal acute wound

All experiments were approved by the Ethical Committee of "Paris-Sud n°26" in accordance with French regulations for animal experiments (#10045-2017052611235636v4). 8-week old NOD/SCID mice were premedicated with subcutaneous injection of 0.05 mg/kg Buprenorphine (Temgesic) and 0.04 mg/kg Atropine (Renaudin) and anesthetized 10 minutes later via intraperitoneal injection of 50 mg/kg Ketamine (Virbac) and 0.5 mg/kg Medetomidine (Domitor). Full-thickness excisional wounds of 1.5 x 1.5 cm^2 were created on the back of each animal. Both sides of Integra Dermal Regeneration Template Single Layers (Integra Lifesciences) were soaked with 50 µL of PBS 1X or a pool of 750,000 NV-MSCs or

IL-MSCs from 7 donors before being grafted on each animal wounds (Figure S6f). Grafted areas were covered with hPBES and protected by a silicon device (Interchim). Mice were left 14 days with the silicon protection before being sacrificed by sedation and overdose of anesthetics according to the French Institutional Animal Guidelines. Wounds were excised, fixed in formalin and embedded in paraffin. Samples were processed for HPS staining and Integrin-β1 (INT-β1), CD206, iNOS, CK-10, COL-4, COL-7, LAM-5 and TNC immunostainings (Supplemental Materials and Methods). hPBES organization and engraftment scores were obtained as described elsewhere (Figure S7).

Statistics

For all experiments, non-parametric Mann-Whitney and Kruskal-Wallis tests were used to determine statistical significance. When necessary, matched or repeated measures were taken into account using non-parametric Friedman test. All charts were plotted as mean ± sem on Prism 6 Graphpad software. Statistical analyses were conducted on R software (3.1.1v). Significance level (*) was set to $p<0.05$.

DATA AVAILABILTY STATEMENT

Datasets related to this article can be found at [http://dx.doi.org/10.17632/4r46w7rfsx.1], hosted at Mendeley Data, v1 (Magne, Brice; Dedier, Marianne; Nivet, Muriel; Coulomb, Bernard; Banzet, Sebastien; Lataillade, Jean-Jacques; Trouillas, Marina (2019), “Table S1. List of the up-regulated proteins found in the secretome of IL-1β primed MSC.”, Mendeley Data, v1

http://dx.doi.org/10.17632/4r46w7rfsx.1).

Journal Pre-proof

ACKNOWLEDGEMENTS

We thank Dr. Sid Ahmed-Adrar from IAL platform for her kind help with the mass spectrometry data collection. We also acknowledge Mr. Casal, Mrs. Auriau and Mr. Peuteman for their kind help with animal care and follow-up. We are also very grateful to Pr. Hovnanian and Mr. Titeux for their kind help to analyze type VII collagen expression. We also thank Mr. Ludovic Dedier for his contribution to data treatment. The PhD of the first author is supported by Scarcell Therapeutics Company, the Fondation Lejeune and the French Government Defense procurement and technology agency.

Disclosure statement

The authors indicate no potential conflicts of interest.

CRediT statement

Conceptualization: BM, BC, MT; Data Curation: BM, MD, MT; Formal analysis: BM, MD, MT; Investigation: BM, MD, MN, MT; Methodology: BM, MT; Visualization: BM, MT; Writing-original draft: BM, MT; Funding acquisition: BC, SB, JJL; Supervision: SB, JJL; Project administration: MT; Validation: MT; Writing – review & editing: MT.

Journal Pre-proof

REFERENCES

Alexaline MM, Magne B, Zuleta Rodriguez A, Nivet M, Bacqueville D, Lataillade JJ, et al. Influence of fibrin matrices and their released factors on epidermal substitute phenotype and engraftment. J Tissue Eng Regen Med 2019.

Alexaline MM, Trouillas M, Nivet M, Bourreau E, Leclerc T, Duhamel P, et al. Bioengineering a human plasma-based epidermal substitute with efficient grafting capacity and high content in clonogenic cells. Stem Cells Transl Med 2015;4(6):643-54.

Auxenfans C, Menet V, Catherine Z, Shipkov H, Lacroix P, Bertin-Maghit M, et al. Cultured autologous keratinocytes in the treatment of large and deep burns: a retrospective study over 15 years. Burns 2015;41(1):71-9.

Benjamin MM, Khalil RA. Matrix metalloproteinase inhibitors as investigative tools in the pathogenesis and management of vascular disease. Exp Suppl 2012;103:209-79.

Cerqueira MT, Frias AM, Reis RL, Marques AP. Boosting and rescuing epidermal superior population from fresh keratinocyte cultures. Stem Cells Dev 2013;23(1):34-43.

Chen D, Hao H, Fu X, Han W. Insight into Reepithelialization: How Do Mesenchymal Stem Cells Perform? Stem Cells Int 2016;2016:6120173.

Chua AW, Khoo YC, Tan BK, Tan KC, Foo CL, Chong SJ. Skin tissue engineering advances in severe burns: review and therapeutic applications. Burns Trauma 2016;4:3.

Cirodde A, Leclerc T, Jault P, Duhamel P, Lataillade JJ, Bargues L. Cultured epithelial autografts in massive burns: a single-center retrospective study with 63 patients. Burns 2011;37(6):964-72.

D'Arpa P, Leung KP. Toll-Like Receptor Signaling in Burn Wound Healing and Scarring. Adv Wound Care (New Rochelle) 2017;6(10):330-43.

de Araujo Farias V, Carrillo-Galvez AB, Martin F, Anderson P. TGF-beta and mesenchymal stromal cells in regenerative medicine, autoimmunity and cancer. Cytokine Growth Factor Rev 2018;43:25-37.

Doucet C, Ernou I, Zhang Y, Llense JR, Begot L, Holy X, et al. Platelet lysates promote mesenchymal stem cell expansion: a safety substitute for animal serum in cell-based therapy applications. J Cell Physiol 2005;205(2):228-36.

Fan H, Zhao G, Liu L, Liu F, Gong W, Liu X, et al. Pre-treatment with IL-1beta enhances the efficacy of MSC transplantation in DSS-induced colitis. Cellular and Molecular Immunology 2012;9(6):473-81.

Fournier BP, Ferre FC, Couty L, Lataillade JJ, Gourven M, Naveau A, et al. Multipotent progenitor cells in gingival connective tissue. Tissue Eng Part A 2010;16(9):2891-9.

Furuyama A, Hosokawa T, Mochitate K. Interleukin-1beta and tumor necrosis factor-alpha have opposite effects on fibroblasts and epithelial cells during basement membrane formation. Matrix Biol 2008;27(5):429-40.

Ganier C, Titeux M, Gaucher S, Peltzer J, Le Lorc'h M, Lataillade JJ, et al. Intradermal Injection of Bone Marrow Mesenchymal Stromal Cells Corrects Recessive Dystrophic Epidermolysis Bullosa in a Xenograft Model. J Invest Dermatol 2018;138(11):2483-6.

Gaur M, Dobke M, Lunyak VV. Mesenchymal Stem Cells from Adipose Tissue in Clinical Applications for Dermatological Indications and Skin Aging. Int J Mol Sci 2015;18(1).

Ge X, Ma X, Meng J, Zhang C, Ma K, Zhou C. Role of Wnt-5A in interleukin-1beta-induced matrix metalloproteinase expression in rabbit temporomandibular joint condylar chondrocytes. Arthritis Rheum 2009;60(9):2714-22.

Glim JE, van Egmond M, Niessen FB, Everts V, Beelen RH. Detrimental dermal wound healing: what can we learn from the oral mucosa? Wound Repair and Regeneration 2013;21(5):648-60.

Gnecchi M, Danieli P, Malpasso G, Ciuffreda MC. Paracrine Mechanisms of Mesenchymal Stem Cells in Tissue Repair. Methods Mol Biol 2016;1416:123-46.

Graves DT, Nooh N, Gillen T, Davey M, Patel S, Cottrell D, et al. IL-1 plays a critical role in oral, but not dermal, wound healing. J Immunol 2001;167(9):5316-20.

Heo SC, Jeon ES, Lee IH, Kim HS, Kim MB, Kim JH. Tumor necrosis factor-alpha-activated human adipose tissue-derived mesenchymal stem cells accelerate cutaneous wound healing through paracrine mechanisms. J Invest Dermatol 2011;131(7):1559-67.

Inman GJ, Nicolas FJ, Callahan JF, Harling JD, Gaster LM, Reith AD, et al. SB-431542 is a potent and specific inhibitor of transforming growth factor-beta superfamily type I activin receptor-like kinase (ALK) receptors ALK4, ALK5, and ALK7. Mol Pharmacol 2002;62(1):65-74.

Jackson WM, Nesti LJ, Tuan RS. Concise review: clinical translation of wound healing therapies based on mesenchymal stem cells. Stem Cells Transl Med 2012;1(1):44-50.

Jeschke MG, Chinkes DL, Finnerty CC, Kulp G, Suman OE, Norbury WB, et al. Pathophysiologic Response to Severe Burn Injury. Annals of Surgery 2008;248(3):387-401.

Kusuma GD, Carthew J, Lim R, Frith JE. Effect of the Microenvironment on Mesenchymal Stem Cell Paracrine Signaling: Opportunities to Engineer the Therapeutic Effect. Stem Cells Dev 2017;26(9):617-31.

Leavitt T, Hu MS, Marshall CD, Barnes LA, Lorenz HP, Longaker MT. Scarless wound healing: finding the right cells and signals. Cell Tissue Res 2016;365(3):483-93.

Lee MJ, Kim J, Kim MY, Bae YS, Ryu SH, Lee TG, et al. Proteomic analysis of tumor necrosis factor-alpha-induced secretome of human adipose tissue-derived mesenchymal stem cells. J Proteome Res 2010;9(4):1754-62.

Li J, Xu SQ, Zhao YM, Yu S, Ge LH, Xu BH. Comparison of the biological characteristics of human mesenchymal stem cells derived from exfoliated deciduous teeth, bone marrow, gingival tissue, and umbilical cord. Mol Med Rep 2018;18(6):4969-77.

Linard C, Tissedre F, Busson E, Holler V, Leclerc T, Strup-Perrot C, et al. Therapeutic potential of gingival fibroblasts for cutaneous radiation syndrome: comparison to bone marrow-mesenchymal stem cell grafts. Stem Cells Dev 2015;24(10):1182-93.

Longmate WM, Dipersio CM. Integrin Regulation of Epidermal Functions in Wounds. Adv Wound Care (New Rochelle) 2014;3(3):229-46.

Macrin D, Joseph JP, Pillai AA, Devi A. Eminent Sources of Adult Mesenchymal Stem Cells and Their Therapeutic Imminence. Stem Cell Rev 2017;13(6):741-56.

Madrigal M, Rao KS, Riordan NH. A review of therapeutic effects of mesenchymal stem cell secretions and induction of secretory modification by different culture methods. J Transl Med 2014;12:260.

Maffioli E, Nonnis S, Angioni R, Santagata F, Cali B, Zanotti L, et al. Proteomic analysis of the secretome of human bone marrow-derived mesenchymal stem cells primed by pro-inflammatory cytokines. J Proteomics 2017;166:115-26.

Magne B, Lataillade JJ, Trouillas M. Mesenchymal Stromal Cell Preconditioning: The Next Step Toward a Customized Treatment For Severe Burn. Stem Cells Dev 2018.

Mah W, Jiang G, Olver D, Gallant-Behm C, Wiebe C, Hart DA, et al. Elevated CD26 Expression by Skin Fibroblasts Distinguishes a Profibrotic Phenotype Involved in Scar Formation Compared to Gingival Fibroblasts. American Journal of Pathology 2017:1-19.

Matsushima K, Bano M, Kidwell WR, Oppenheim JJ. Interleukin 1 increases collagen type IV production by murine mammary epithelial cells. J Immunol 1985;134(2):904-9.

Mauviel A, Lapiere JC, Halcin C, Evans CH, Uitto J. Differential cytokine regulation of type I and

type VII collagen gene expression in cultured human dermal fibroblasts. J Biol Chem 1994;269(1):25-8.

McBride JD, Rodriguez-Menocal L, Candanedo A, Guzman W, Garcia-Contreras M, Badiavas EV. Dual mechanism of type VII collagen transfer by bone marrow mesenchymal stem cell extracellular vesicles to recessive dystrophic epidermolysis bullosa fibroblasts. Biochimie 2018;155:50-8.

Monaco S, Sparano V, Gioia M, Sbardella D, DiPierro D, Marini S, et al. Enzymatic processing of collagen IV by MMP-2 (gelatinase A) affects neutrophil migration and it is modulated by extracatalytic domains. Protein Science 2006;15:2805-15.

Orozco A, Gemmell E, Bickel M, Seymour GJ. Interleukin-1beta, interleukin-12 and interleukin-18 levels in gingival fluid and serum of patients with gingivitis and periodontitis. Oral Microbiol Immunol 2006;21(4):256-60.

Park SR, Kim JW, Jun HS, Roh JY, Lee HY, Hong IS. Stem Cell Secretome and Its Effect on Cellular Mechanisms Relevant to Wound Healing. Mol Ther 2018;26(2):606-17.

Pasternak B, Aspenberg P. Metalloproteinases and their inhibitors-diagnostic and therapeutic opportunities in orthopedics. Acta Orthop 2009;80(6):693-703.

Peplow PV, Chatterjee MP. A review of the influence of growth factors and cytokines in in vitro human keratinocyte migration. Cytokine 2013;62(1):1-21.

Preshaw PM, Taylor JJ. How has research into cytokine interactions and their role in driving immune responses impacted our understanding of periodontitis? J Clin Periodontol 2011;38 Suppl 11:60-84.

Qi Y, Jiang D, Sindrilaru A, Stegemann A, Schatz S, Treiber N, et al. TSG-6 released from intradermally injected mesenchymal stem cells accelerates wound healing and reduces tissue fibrosis in murine full-thickness skin wounds. J Invest Dermatol 2014;134(2):526-37.

Redondo-Castro E, Cunningham CJ, Miller J, Brown H, Allan SM, Pinteaux E. Changes in the secretome of tri-dimensional spheroid-cultured human mesenchymal stem cells in vitro by interleukin-1 priming. Stem Cell Res Ther 2018;9(1):11.

Seeger MA, Paller AS. The Roles of Growth Factors in Keratinocyte Migration. Advances in Wound Care (New Rochelle) 2015;4(4):213-24.

Singer AJ, Clark RA. Cutaneous wound healing. N Engl J Med 1999;341(10):738-46.

Song Y, Dou H, Li X, Zhao X, Li Y, Liu D, et al. Exosomal miR-146a Contributes to the Enhanced Therapeutic Efficacy of Interleukin-1beta-Primed Mesenchymal Stem Cells Against Sepsis. Stem Cells 2017;35(5):1208-21.

Stanojcic M, Abdullahi A, Rehou S, Parousis A, Jeschke MG. Pathophysiological Response to Burn Injury in Adults. Ann Surg 2018;267(3):576-84.

Sun J, Chen J, Cao J, Li T, Zhuang S, Jiang X. IL-1beta-stimulated beta-catenin up-regulation promotes angiogenesis in human lung-derived mesenchymal stromal cells through a NF-kappaB-dependent microRNA-433 induction. Oncotarget 2016;7(37):59429-40.

Takeda A, Kadoya K, Shioya N, Uchinuma E, Tsunenaga M, Amano S, et al. Pretreatment of human keratinocyte sheets with laminin 5 improves their grafting efficiency. J Invest Dermatol 1999;113(1):38-42.

Ter Horst B, Chouhan G, Moiemen NS, Grover LM. Advances in keratinocyte delivery in burn wound care. Adv Drug Deliv Rev 2018;123:18-32.

Tomar GB, Srivastava RK, Gupta N, Barhanpurkar AP, Pote ST, Jhaveri HM, et al. Human gingiva-derived mesenchymal stem cells are superior to bone marrow-derived mesenchymal stem cells for cell therapy in regenerative medicine. Biochemical and Biophysical Research Communications 2010;393(3):377-83.

Vardar-Sengul S, Arora S, Baylas H, Mercola D. Expression profile of human gingival fibroblasts

induced by interleukin-1beta reveals central role of nuclear factor-kappa B in stabilizing human gingival fibroblasts during inflammation. Journal of Periodontology 2009;80(5):833-49.

Zhang B, Wang M, Gong A, Zhang X, Wu X, Zhu Y, et al. HucMSC-exosome mediated -Wnt4 signaling is required for cutaneous wound healing. Stem Cells 2014.

Zhang B, Wu X, Zhang X, Sun Y, Yan Y, Shi H, et al. Human Umbilical Cord Mesenchymal Stem Cell Exosomes Enhance Angiogenesis Through the Wnt4/beta-Catenin Pathway. Stem Cells Transl Med 2015.

Journal Pre-proof

Journal Pre-proof

FIGURE LEGENDS

Figure 1. IL-1β-primed MSCs improve wound closure, epidermal maturation and reduce inflammation *in vitro*. (a) Wound closure percentage at 5h of TOX, co-cultured in inserts with NV- or IL-MSCs (ratio to TOX, n=8). (b) Hematoxylin-Phloxin-Safranin stainings , epidermal layer number, basal organization score, and (c) IHC stainings of hPBES (CTRL) co-cultured with NV- or IL-MSCs (n=7). (d) Dosage of IL-1RA and (e) TNF-α in the supernatants of LPS-challenged THP-1 co-cultured for 24h with NV- or IL-MSCs (ratio to LPS, n=6). Scale bar = 50 (a), 100 (b) μm. Values are expressed as means± SEM. *p<0.05; **p<0.01; ns, not significant; CK-10, Cytokeratin-10; COL-4, Collagen-4; CTRL, control; hPBES, human Plasma-based Epidermal Substitute; IL, IL-1β; LAM-5, Laminin-5; MSC, mesenchymal stromal cells; NV, naive; TNC, Tenascin-C; TOX, intoxicated keratinocytes.

Figure 2. IL-1β-primed MSCs stimulate hPBES engraftment and epidermal maturation *in vivo*. (a) Reepithelialization scores are expressed as a percentage of mice present in each reepithelialization groups (bad: 0-20%, medium: 20-60%, good: 60-100%). (b) Hematoxylin-Phloxin-Safranin stainings, epidermal layer number, basal organization score, (c) IHC stainings and (d) marker quantifications of hPBES (CTRL) at 14 days after *in vivo* grafting and treatment with NV- or IL-MSCs (scale bar = 100 μm) (n=10 to 16). Values are expressed as means ± SEM. * p<0.05; ** p<0.01; ns, not significant; CK-10, Cytokeratin-10; COL-4, Collagen-4; CTRL, control; hPBES, human Plasma-based Epidermal Substitute; IL, IL-1β; LAM-5, Laminin-5; MSC, mesenchymal stromal cells; NV, naive; TNC, Tenascin-C.

Figure 3. Naive and IL-1β-primed MSCs possess distinct secretory profiles. (a) Protein repartition, and (b) intensity score analysis in NV- and IL-CM using mass spectrometry

analysis (n=7 donors). (c) ELISA dosages of selected wound healing-related proteins in NV- and IL-CM used at 10µg/ml (n=7 donors). Values are expressed as means ± SEM. * p<0.05; ** p<0.01; ns, not significant; A.U., Arbitrary units; IL, IL-1β; MSC, mesenchymal stromal cells; NV, naive.

Figure 4. IL-1β-primed MSC Conditioned Medium improves skin wound healing *in vitro*. (a) Wound closure at 5h of TOX, cultured with NV- or IL-CM (scale bar = 500µm) (ratio to TOX, n=7). (b) Nidogen-1, (c) Tenascin-C and (d) Laminin-γ2 expression assessed by western blot at 8 days of keratinocyte and fibroblast co-cultures (CTRL) grown with NV- or IL-CM (ratio to control, n=7). (e) Dosage of TNF-α and (f) IL-1RA in the supernatants of LPS-challenged THP-1 cultured for 24h with NV- or IL-CM (ratio to LPS, n=10 to 16). Values are expressed as means ± SEM. * p<0.05; ** p<0.01; *** p<0.001; ns, not significant; CM, conditioned medium; CTRL, control; IL, IL-1β; LAM-γ2, Laminin-5 γ2 chain; NID-1, Nidogen-1; NV, naive; TNC, Tenascin-C; TOX, intoxicated keratinocytes.

Figure 5. IL-1β-primed MSCs positively impact skin wound healing via TGF-β1 and MMPs *in vitro*. (a-b) Wound closure at 5h of TOX (scale bar = 500µm) (ratio to TOX, n=7 to 8), (c-h) Nidogen-1, Laminin-γ2 and Tenascin-C protein expression assessed by western blot at 8 days in keratinocyte and fibroblast (CTRL) cultures (ratio to CTRL, n=6 to 7) and (i-l) dosage of TNF-α and IL-1RA in supernatants of LPS-challenged THP-1 cultured for 24h (ratio to LPS, n=5 to 19), grown or not with (a-c-d-e-i-k) SB431542- or Tigecycline-supplemented IL-CM, or (b-f-g-h-j-l) selected IL-CM-derived factors. Values are expressed as means± SEM. *p<0.05; **p<0.01; ***p<0.001; ns, not significant. CM, conditioned medium; CTRL, control; IL, IL-1β; LAM-γ2, Laminin-5 γ2 chain; NID-1, Nidogen-1; NV,

naive; TNC, Tenascin-C; TOX, intoxicated keratinocytes.

Figure 6. Summary of the main findings. IL-MSCs mediate keratinocyte migration, differentiation, DEJ deposition and mitigate inflammation of THP1 cells through the release of MMP-1, MMP-9, TGF-β1, IGFBP-7 and HGF *in vitro*. They further improve skin wound healing and hPBES engraftment *in vivo*. CK-10, Cytokeratin-10; COL-4, Collagen-4; DEJ, dermal-epidermal junction; hPBES, human Plasma-based Epidermal Substitute; KC, keratinocyte; LAM-5, Laminin-5; MSC, mesenchymal stromal cells; NID-1, Nidogen-1; TNC, Tenascin-C.

Journal Pre-proof

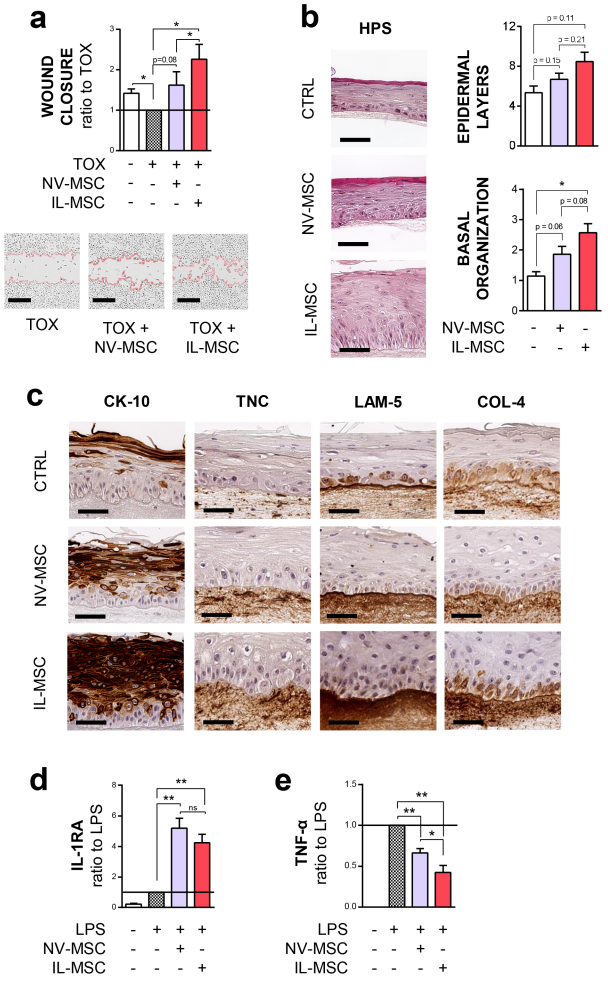
a
WOUND CLOSURE ratio to TOX
p=0.08
TOX - + + +
NV-MSC - - + -
IL-MSC - - - +
TOX
TOX + NV-MSC
TOX + IL-MSC
b
HPS
CTRL
NV-MSC
IL-MSC
EPIDERMAL LAYERS
p = 0.11
p = 0.21
p = 0.15
BASAL ORGANIZATION
p = 0.08
p = 0.06
NV-MSC - + -
IL-MSC - - +
c
CK-10
TNC
LAM-5
COL-4
CTRL
NV-MSC
IL-MSC
d
IL-1RA ratio to LPS
ns
LPS - + + +
NV-MSC - - + -
IL-MSC - - - +
e
TNF-α ratio to LPS
LPS - + + +
NV-MSC - - + -
IL-MSC - - - +

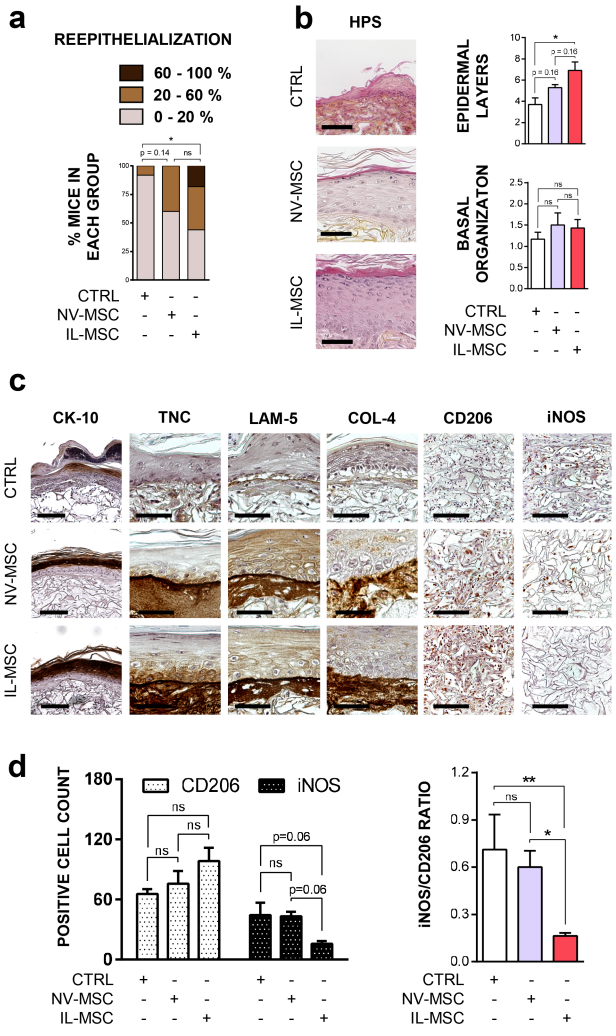
a
REEPITHELIALIZATION
60 - 100 %
20 - 60 %
0 - 20 %
% MICE IN EACH GROUP
p = 0.14
ns
CTRL + - -
NV-MSC - + -
IL-MSC - - +
b
HPS
CTRL
NV-MSC
IL-MSC
EPIDERMAL LAYERS
p = 0.16
p = 0.16
BASAL ORGANIZATON
ns
ns
ns
CTRL + - -
NV-MSC - + -
IL-MSC - - +
c
CK-10
TNC
LAM-5
COL-4
CD206
iNOS
CTRL
NV-MSC
IL-MSC
d
POSITIVE CELL COUNT
CD206
iNOS
ns
ns
ns
p=0.06
ns
p=0.06
CTRL + - - + - -
NV-MSC - + - - + -
IL-MSC - - + - - +
iNOS/CD206 RATIO
**
ns
*
CTRL + - -
NV-MSC - + -
IL-MSC - - +

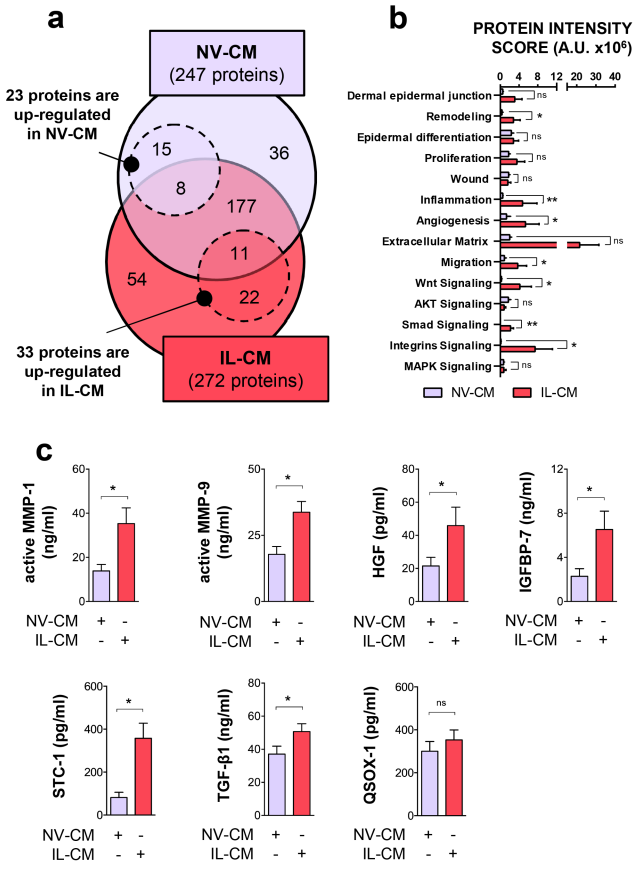

Journal Pre-proof

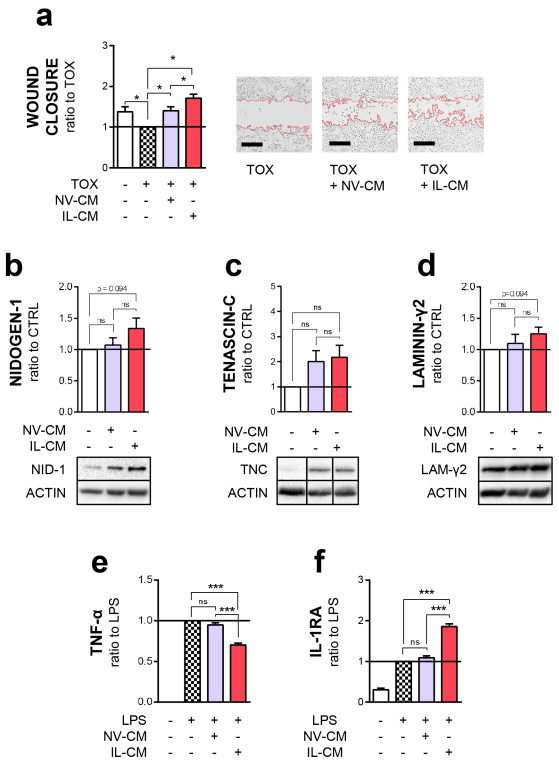

Journal Pre-proof

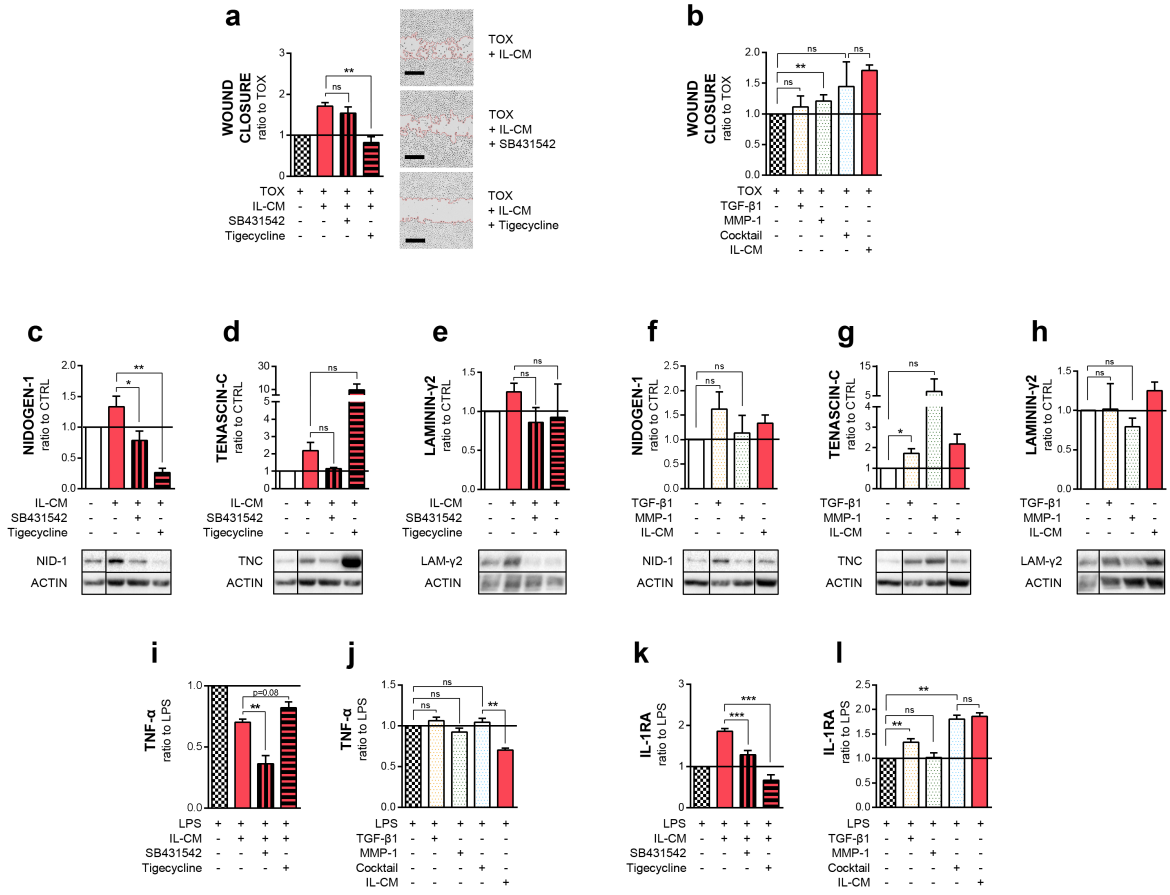
a
WOUND CLOSURE ratio to TOX
TOX + IL-CM
TOX + IL-CM + SB431542
TOX + IL-CM + Tigecycline
TOX
IL-CM
SB431542
Tigecycline
b
WOUND CLOSURE ratio to TOX
TOX
TGF-β1
MMP-1
Cocktail
IL-CM
c
NIDOGEN-1 ratio to CTRL
IL-CM
SB431542
Tigecycline
NID-1
ACTIN
d
TENASCIN-C ratio to CTRL
TNC
e
LAMININ-γ2 ratio to CTRL
LAM-γ2
f
NIDOGEN-1 ratio to CTRL
g
TENASCIN-C ratio to CTRL
h
LAMININ-γ2 ratio to CTRL
i
TNF-α ratio to LPS
p=0.08
LPS
j
TNF-α ratio to LPS
k
IL-1RA ratio to LPS
l
IL-1RA ratio to LPS

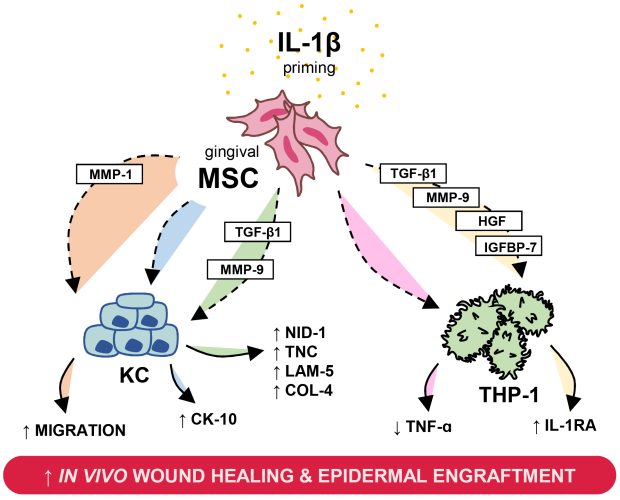

Journal Pre-proof

Supplemental Materials and Methods

Journal Pre-proof

MSC isolation and culture

Gingival biopsies of 7 healthy human donors were cut and digested for 2.5 hours at 37 °C with 2.4 U/mL dispase II (Roche), 0.8 U/mL collagenase MTF (Roche), 100 IU/mL penicillin (Panpharma), 50 µg/mL gentamicin (Panpharma), 2,5 µg/mL amphotericin B (Bristol-Myers Squibb). Harvested cells were seeded at 5,000 cells/cm² and cultivated in MEMα culture medium supplemented with 5% human platelet lysate (PL), 2 IU/mL heparin (Sanofi), 100 IU/mL penicillin, 50 µg/mL gentamicin and 2.5 µg/mL amphotericin B at 37 °C in a humid atmosphere under 5% CO2. After 2 days, cell medium was changed and amphotericin B was reduced to 1 µg/mL. Cells were trypsinized at 80% confluence using 0.05% trypsin/EDTA (Gibco) for 5 minutes at 37 °C and replated between 4,000 and 5,000 cells/cm^2 or frozen in a mixture of MEMα, 10% DMSO (Sigma) and 9 % human serum albumin (LFB Biomedicaments).

Keratinocyte isolation and culture

Human keratinocytes and dermal fibroblasts were obtained after informed consent from healthy donors undergoing breast reduction surgery. Skin pieces were digested overnight at 4°C in 1.8 UI/mL dispase II and 0.0625 % trypsin (Biochrom). After mechanical separation from the dermis, the epidermis was dissociated at 37°C in 0.05 % trypsin/EDTA (Gibco) for 30 min. Keratinocytes were immediately frozen. Dermis was digested in 2.4 UI/mL dispase II and 2.4 mg/mL collagenase II. Harvested dermal fibroblasts were plated at 4,000 cells/cm² and amplified in DMEM (Gibco) supplemented with 5% human PL, 10 µg/ml ciprofloxacin (Bayer Pharma) and 2 UI/ml heparin. At 80% confluence, fibroblasts were frozen in liquid nitrogen. Keratinocytes were thawed and plated at 2,400cells/cm² on a growth-arrested irradiated fibroblast feeder layer (60 Grays of γ rays), seeded at 20,000 cells/cm² in a medium described elsewhere {Alexaline, 2015 #205}. Medium change was performed every two to three days. Before reaching 70% confluence, keratinocytes were trypsinized and used for wound closure assay, DEJ formation assay or hPBES preparation.

Human Plasma-Based Epidermal Substitute (hPBES) preparation

hPBES were prepared as described previously {Alexaline, 2015 #205}. Briefly, a mix solution containing 39.8 % of plasma (pool of fresh frozen human plasma, obtained from 10 donors), 4.66 mg/mL NaCl (Fresenius), 0.8mg/ml Calcium Chloride (Laboratoire Renaudin) and 0.39 mg/mL Exacyl (Sanofi) was poured on appropriate culture plates (0.3 mL/cm²) and left to polymerize for minimum 3 h at 37°C. Growth-arrested fibroblasts and keratinocytes were then plated on this plasma matrix at 20,000 cells/cm^2 and 2,400 cells/cm^2 respectively. After 14 days of culture, epidermal substitutes were used for *in vitro* air/liquid differentiation assay or *in vivo* grafting.

Flow cytometry

MSCs were incubated with primary antibodies diluted in a PBS solution containing 2% w/v human serum albumin and 0.5% w/v human immunoglobulin G (LFB Biomedicaments) for 20 min at 4°C. Primary antibodies included anti-CD45-FITC, anti-CD90-FITC, anti-HLA-DR-FITC, anti-CD44-PE, anti-CD105-PE, anti-CD73-PE, anti-CD29-PE, anti-IgG1-FITC or PE (all from Beckman Coulter). After PBS washing, stained MSCs were analyzed using flow cytometry (Beckman Coulter Navios). Isotypic control was used as a negative control.

Differentiation Assays

For osteogenic differentiation assay, MSCs were seeded at 3,000 cells/cm^2 and cultured for 21 days in MEMα supplemented with 10% FCS, 0.1µM dexamethasone, 0.05mM L-ascorbic acid-2-phosphate and 10mM -glycerophosphate (all from Sigma), with medium change 2 to 3 times a week. Matrix mineralization was assessed using a 2% Alizarine Red (AR) solution (Sigma). It was further confirmed by a Von Kossa (VK) staining, incubating the cells for 15 min under UV-light in a 1% silver nitrate solution. For chondrogenic differentiation assay, MSCs were pelleted at 500g for 5min without brake and cultured for 21 days in DMEM high Glucose (Gibco) supplemented with 10% FCS, 1 mM sodium pyruvate, 0.35 mM L-proline, 1X ITS, 0.17 mM ascorbic acid-2-phosphate, 0.1 µM dexamethasone, 10 ng/ml TGF-β3 (all from Sigma) and 5.3µg/ml linoleic acid (Fluka). Pellets were embedded in paraffin and glycosaminoglycans were identified with Alcian Blue staining (VWR). For adipogenic differentiation assay, sub-confluent cultures of MSCs were exposed to three induction cycles with a medium composed of MEMα supplemented with 10% FCS, 1 µM dexamethasone, 0.5 mM 3-isobuthyl-1-methylxanthine, 10 µM insulin, 200 µM indomethacin (all from Sigma). After 21 days, lipid droplets were stained using an Oil red O (ORO) solution (Cayman Chemical).

Mass spectrometry and secretome analysis

18 µg of NV-CM and IL-CM were pseudo-separated by 10% SDS-polyacrylamide gel electrophoresis. Proteins were reduced, alkylated, and digested in gel using a DigestPro instrument (Intavis, Koeln) according to manufacturer's instructions. Tryptic peptides were then dried in a vacuum centrifuge (Vacuum Concentrator, Thermoscientific) and analyzed by high performance liquid chromatography (HPLC) tandem mass spectrometry (LTQ-Orbitrap Velos, Thermoscientific). 2µL of peptides were injected in the system using a pre-concentration column (Acclaim PepMap C18, Thermoscientific), and separated by reversed phase chromatography using a C18 column (Acclaim PepMap nanoViper C18, Thermoscientific). Separation was achieved in a linear 45 min LC gradient from 4% to 55% acetonitrile in 0.1% formic acid (v/v) at a flow rate of 250 nL/min before direct electrospraying into the mass spectrometer. Raw MS file were processed with Proteome Discoverer (1.4v). Peak list files were searched using SEQUEST against the human SwissProt protein database (released on Sep 2017). The search included variable modifications for oxidation of methionine, peptide N-terminal acetylation and Carbamidomethylation of cysteine was set as a fixed modification. Peptides were matched using trypsin as a digestion enzyme and one miss cleavage site was allowed. The mass error for the precursor ions (full MS) was less than 10 ppm (errorppm = (m/zexperimental - m/zexact) x 106/ m/zexact). Mass error for ions from the MS/MS spectra was reported less than 0.6 Da. Peptides mass is searched between 350 Da and 7000 Da with time retention from 10 min to 60 min. Peptide identifications were validated by determination of false positives by target decoy PSM validator. It is high if the false positive rate (FDR or false Discovery rate) is less than 1%, low if the FDR is greater than 5% and average (medium between 1 and 5 %). Peptide identification Xcorr were calculated by the correlation of MS/MS experimental spectrum compared with the theoretical MS/MS spectrum generated by the Proteome Discoverer 1.4 software.

Impurities (such as serum albumin or keratins) were removed from our data analysis. A Venn's diagram was drawn according to the presence, absence or overexpression of proteins in NV- and IL-CM of n=7 donors of MSCs. Overexpression was established using a paired Wilcoxon test. Significantly differentially expressed proteins were then classified depending on their biological function in one or several of the following categories: "DEJ", "remodeling", "epidermal differentiation", "proliferation", "wound healing", "inflammation", "angiogenesis", "ECM", "migration", "AKT signaling", "Smads signaling", "integrin signaling", "Wnt Signaling" and "MAPK signaling". To help classify proteins, we used the Go Quick data base (https://www.ebi.ac.uk/QuickGO/) which associates proteins and GOTERMS. After establishing which GOTERMS correspond to which category (Table S2), we were able to classify all overexpressed proteins. For each category, we then calculated a mean protein intensity score for NV- and IL-CM. Interaction between selected identified proteins and target mediators were also studied using the String online database (https://string-db.org/).

Western blots

Cells were lysed in a PBS solution containing 1% NP40, 0.1 % of SDS, 0.5 % of deoxycholic acid, protease and phosphatase inhibitor cocktails (all from Sigma). Supernatants were collected after centrifugation at 13,000 g for 15min.Total protein content in cell lysates was evaluated with Bio-rad Protein Assay kit. 50 µg of protein samples were loaded on 10% SDS-polyacrylamide gels (Bio-Rad). After 45min of migration, proteins were electro-transferred at 4°C for 2.5hours on PVDF membrane (Immobilon-P Transfer Membrane, Millipore). Membranes were blocked at room temperature for 2 h in PBS 2% Tween 20 (Sigma) and 3% skimmed milk and incubated overnight at 4°C with primary antibodies (see table below). Membranes were then incubated for 45 min with horseradish peroxidase (HRP)-conjugated goat anti-rabbit, goat anti-mouse or donkey anti-goat immunoglobulin G (IgG) (Santa-Cruz). ECL substrate (Bio-Rad) was used to reveal antibody-binding sites. Signal intensity was detected with Chemidoc instrument and analyzed with Image Lab software. Then, signal intensity of protein of interest was normalized to signal intensity of β-actin.

Antibody	Blocking buffer	Clone or reference	Dilution	Supplier
β-actin	skimmed milk	ab8227	1/1000	Abcam
Laminin 5 gamma chain 2	skimmed milk	#D4B5	1/800	Merck Millipore
Nidogen	skimmed milk	#AF2570	1/500	Novus Biologicals
Tenascin C	skimmed milk	#4C8MS	1/1000	Novus Biologicals

Histology, Immunohistochemistry (IHC), quantification and scoring

Samples were washed in PBS, fixed in 4 % formalin (LaboNord) and dehydrated with graded series of ethanol solutions prior to paraffin embedding (Thermo Scientific). Paraffin sections of 5 µm thickness were dried, deparaffinized, and stained with Hematoxylin-Phloxin-Safranin (HPS) (All from Dako). For IHC, paraffin sections of 5µm thickness were fixed on polylysine slides (Thermo Scientific). Sections were dried overnight at 37°C and deparaffinized. Antigen retrievals were performed in pH 6 solution for 20 min at 95°C, pH 9 solution for 20 min at 95°C, 0.1 mg/ml $CaCl_2$ solution containing 1 mg/ml pronase (Sigma) for 10 min at 37°C, or 1 % trypsin (Gibco) for 30 min at 37°C. Endogenous peroxidases were blocked with 3 % H_2O_2 (Dako, Denmark). Sections were incubated at room temperature for 30 minutes with primary antibodies (see table below). Detection was performed using LSAB™2 Kit (Dako) with Dako autostainer instrument.

Antibody	Antigen retrieval	Clone or reference	Dilution	Supplier
CD206	pH6	#ab64693	1/500	Abcam
CK10	pH9	#DE-K10	1/50	Dako
Collagen IV	1mg/ml pronase (Sigma) for 10min at 37°C	ab6586	1/600	Abcam
Collagen VII	4mg/ml Pepsin for 30min at 37°C	#LH7.2	1/100	Sigma
iNOS	pH6	ab15323	1/50	Abcam
Integrin β1	pH6	#4B7R	1/100	Abcam
Laminin 5	1mg/ml pronase (Sigma) for 10min at 37°C	#P3H9	1/600	Abcam
Tenascin C	1% trypsin (Gibco) for 30 min at 37°C	#4C8MS	1/200	Novus Biological

M1-to-M2 ratio was calculated as the ratio of iNOS positive cell count to CD206 positive cell count. Basal layer organization and epidermal layer number were obtained from three observers. Basal organization was considered the best when nuclei reached an apical position, keratinocytes appeared cuboidal and no discontinuity in the basal layer was observed (Figure S2a). Human reepithelialization percentage was calculated as the ratio of human Integrin-β1 positive epidermal length to total wound length (Figure S2b).

Journal Pre-proof

Table S1. List of the up-regulated proteins found in the secretome of IL-1β primed MSC.

Protein Name	Molecular function	Biological Process	Significance	Intensity ratio
Collagen alpha-1(VII) chain	ECM structural constituent	ECM organization. Cell adhesion	0.0075	Appearance
Growth-regulated alpha protein	Signaling receptor binding	Inflammation. Cell communication and trafficking	0.0075	Appearance
Interleukin-6	Cytokine activity	Immune response	0.0075	Appearance
Superoxide dismutase [Mn]. mitochondrial	Metal ion binding	Oxidation-reduction process. Stress response	0.0075	Appearance
Thrombospondin-2	ECM structural constituent	Cell adhesion. Angiogenesis. Collagen assembly	0.0075	Appearance
CD44 antigen	Hyaluronic acid binding	Cell adhesion. Migration	0.0211	Appearance
Complement factor B	Complement binding	Complement activation	0.0211	Appearance
Prolow-density lipoprotein receptor-related protein 1	Apolipoprotein binding	Cell proliferation. Migration. Lipid metabolism. Endocytosis	0.0211	Appearance
Procollagen-lysine.2-oxoglutarate 5-dioxygenase 2	Metal ion binding	ECM remodeling. Oxidation-reduction process	0.0211	Appearance
Glutaminyl-peptide cyclotransferase	Glutaminyl-peptide cyclotransferase activity	CCL2 formation and monocyte infiltration. Inflammation	0.0211	Appearance
Vasorin	Protein binding	Inhibitor of mature TGF Growth factor. Migration	0.0211	Appearance
Stromelysin-1	Metallopeptidase activity	ECM remodeling	0.0341	342.1661
Calsyntenin-1;Soluble Alc-alpha;CTF1-alpha	Calcium ion binding	Regulation of post-synaptic calcium concentration	0.0545	5.5729
Endoplasmin	Calcium ion binding	Chaperone protein. regulation of innate and adaptative immunity	0.0545	17.1756
Stanniocalcin-1	Hormone activity	Inflammation. Anti-apoptotic. Angiogenesis. Migration	0.0562	5.6148
Peroxidasin homolog	ECM structural constituent	ECM organization. Immune response. Oxidation-reduction process	0.0591	11.5382
Calreticulin	Protein binding	Stress response. inflammation	0.0636	Appearance
Adenylyl cyclase-associated protein	Actin binding	Migration	0.0636	Appearance
F-actin-capping protein subunit alpha-1	Actin binding	Actin filament capping	0.0636	Appearance
CD109 antigen	Transforming Growth Factor beta binding	Regulation of keratinocytes differentiation	0.0636	Appearance
Collagen alpha-2(IV) chain	ECM structural constituent	ECM organization. Angiogenesis Appearance	0.0636	Appearance
Peptidyl-prolyl cis-trans isomerase FKBP10	Calcium ion binding	Stress response. Angiogenesis. Migration. Pro-collagen maturation	0.0636	Appearance
Follistatin	Activin binding	Inhibitor of mature TGF. Positive regulation of hair follicle development	0.0636	Appearance
Malate dehydrogenase. cytoplasmic	L-malate deshydrogenase activity	Oxidation-reduction process. Gluconeogenesis	0.0636	Appearance
Retrotransposon gag domain-containing protein 4	Neofunctionalized retrotransposons gene		0.0636	Appearance
Serpin B6	Protease binding	Cellular response to osmotic stress. Inhibitor of cathepsin G. kallikrein-8 and thrombin	0.0636	Appearance
Tripartite motif-containing protein 67	Metal ion binding	Neuronal differentiation	0.0636	Appearance
Nucleobindin-1	Calcium ion binding	Cellular protein metabolic process	0.0670	7.3019
Caveolin-1;Caveolin	Protein binding	Angiogenesis. Cellular response to transforming growth factor beta	0.0765	5.5652
Proteasome subunit beta type-2	Threonine-type endopeptidase activity	Stress response. Proteolytic degradation of intracellular protein	0.0907	1.3182
Proteasome subunit beta type-3	Threonine-type endopeptidase activity	Proteolytic degradation of intracellular protein	0.1000	2.3290
Spondin-2	Antigen. lipopolysaccharide or metal ion binding	Cell adhesion. Innate immune response	0.1031	2.5641
Insulin-like growth factor-binding protein 4	Insulin-like growth factor binding	Inflammatory response. Cell growth.	0.1235	3.5880
Heat shock cognate 71 kDa protein	ATPase activity. Chaperonne binding	Stress response	0.1388	18.1507
Vitronectin	ECM structural constituent. heparin binding	Cell adhesion. migration	0.1435	16.0781
Prelamin-A/C	Protein binding	Nuclear assembly. Chromatin organization. Nuclear membrane and telomere dynamics	0.1594	1.4006
Latent-transforming growth factor beta-binding protein 1	Transforming growth factor beta-activated receptor activity	TGF-beta activation	0.1705	10.5934
Fibulin-1	ECM structural constituent. calcium ion and fibrinogen binding	Cell adhesion and migration. Organization of ECM architecture	0.1732	5.6942
Serpin H1	Serine-type endopeptidase inhibitor activity. collagen binding	Chaperone in the biosynthetic pathway of collagen	0.1732	6.8382
Heat shock 70 kDa protein 1B	ATPase activity. Chaperone activity	Stress response	0.1840	1.5424
Annexin A5;Annexin	Calcium ion and heparin binding	Anticoagulant activity	0.2000	10.1960
Phosphoglycerate mutase 1	Bisphosphoglycerate mutase and hydrolase activity	Glycolysis	0.2045	2.4965
Beta-actin-like protein 2	Structural molecule activity	Cell cycle. Endocytosis. Exocytosis. Intracellular protein transport	0.2186	3.8955
Target of Nesh-SH3	Collagen and heparin binding	ECM organization	0.2207	Appearance
Aldose reductase	Oxidoreductase activity. NAD or NADP as acceptor	Oxidation-reduction process	0.2207	Appearance
Aminopeptidase N	Metallopeptidase activity. Peptide and zinc ion binding	Cellular catabolic process. Angiogenesis	0.2207	Appearance
V-type proton ATPase subunit C 2	ATPase activity	ATP hydrolysis coupled proton transport. phagosome acidification	0.2207	Appearance
Calumenin	Calcium ion binding	Cellular protein metabolic process	0.2207	Appearance
Macrophage-capping protein	Actin binding. Structural molecule activity	Macrophage function	0.2207	Appearance
Centrosomal protein of 290 kDa	Protein binding	Protein transport	0.2207	Appearance
C-X-C motif chemokine;Interleukin-8	Cytokine activity	Inflammatory response	0.2207	Appearance
Endoplasmic reticulum aminopeptidase 1	Metallopeptidase activity. Peptide and zinc ion binding	Immune response. Angiogenesis	0.2207	Appearance
ERI1 exoribonuclease 2	3'-5'-exodeoxyribonuclease activity		0.2207	Appearance
Glutaredoxin-3	Metal ion binding	cellular iron ion homeostasis	0.2207	Appearance
C-type mannose receptor 2	transmembrane signaling receptor activity	Remodeling ECM	0.2207	Appearance
Nidogen-1	ECM Structural component. ECM binding	ECM and basement membrane organization	0.2207	Appearance
Nidogen-2	ECM Structural component. ECM	ECM and basement membrane organization	0.2207	Appearance

Journal Pre-proof

Journal Pre-proof

	binding			
Perilipin-3	Cadherin binding	Vesicle-mediated transport	0.2207	Appearance
Plastin-3	Actin filament and calcium binding	Actin filament bundle assembly	0.2207	Appearance
Plasma protease C1 inhibitor	Serine-type endopeptidase inhibitor activity	Complement activation. Blood coagulation. fibrinolysis	0.2207	Appearance
Staphylococcal nuclease domain-containing protein 1	Endonuclease activity	RNA catabolic process	0.2207	Appearance
Sushi repeat-containing protein SRPX	protein binding	Urokinase plasminogen activator surface receptor. Angiogenesis. Cell migration and adhesion	0.2207	Appearance
Sushi. von Willebrand factor type A. EGF and pentraxin domain-containing protein 1	Calcium ion and chromatin binding	Cell adhesion	0.2207	Appearance
Tripeptidyl-peptidase 1	Serine-type endopeptidase activity	Protein catabolic process	0.2207	Appearance
Ubiquitin-like modifier-activating enzyme 1	Ubiquitin activating enzyme activity	Protein ubiquitination	0.2207	Appearance
Actin-related protein 2/3 complex subunit 4	Actin binding	actin filament polymerization	0.2359	2.0205
Mannan-binding lectin serine protease 1	Peptidase activity. Calcium-dependent protein and calcium ion binding	Complement activation	0.2449	15.9472
Complement C4-B	Endopeptidase inhibitor activity. Complement binding	Complement activation. Inflammatory response	0.2454	4.2798
Laminin subunit gamma-1	ECM Structural component	Cell adhesion. Migration. Hemidesmosome assembly	0.2492	4.1333
Plasminogen	serine-type endopeptidase activity	Fibrinolysis. Inflammation. Tissue remodeling	0.2492	2.9851
Latent-transforming growth factor beta-binding protein 2	Calcium ion binding	Elastic-fiber architectural organization and/or assembly	0.2496	1.1707
Rab GDP dissociation inhibitor beta	GTPase activator activity	Vesicle-mediated transport	0.2946	4.8105
Apolipoprotein A-I	Apolipoprotein receptor binding	Cellular protein metabolic process	0.3013	2.2368
Insulin-like growth factor-binding protein 2	Insulin-like growth factor binding	Regulation of insulin-like growth factor receptor signaling pathway	0.3045	2.2418
Insulin-like growth factor-binding protein 7	Insulin-like growth factor binding	Cell adhesion. Inflammation. Regulation of insulin-like growth factor receptor signaling pathway	0.3062	9.4905
Thrombospondin-1	ECM structural component	ECM organization. Immune response. Cell migration and adhesion	0.3062	3.3088
Biglycan	ECM Structural component. ECM binding	ECM organization	0.3094	2.6493
Pentraxin-related protein PTX3	Complement component C1q binding	Inflammatory response	0.3095	3.5025
F-actin-capping protein subunit beta	Actin filament binding	Cytoskeleton organization. Endoplasmic reticulum to Golgi vesicle-mediated transport	0.3333	1.8726
Serum amyloid P-component	Low-density lipoprotein particle binding	Immune response. Scavenge nuclear material released from damaged circulating cells	0.3537	1.8092
Collagen triple helix repeat-containing protein 1	Frizzled binding. Wnt-protein binding	Negative regulator of collagen matrix deposition	0.3537	15.0583
Annexin A2	Calcium-dependent protein binding	Heat-stress response. Angiogenesis	0.3690	2.9617
C-type lectin domain family 11 member A	Growth factor activity	Positive regulation of proliferation	0.3690	2.8880
Complement factor H	Heparin binding	Complement activation	0.3751	6.0051
Glyceraldehyde-3-phosphate dehydrogenase	Glyceraldehyde-3-phosphate dehydrogenase (NAD+) (phosphorylating) activity	Apoptosis. Glycolysis. Translation regulation	0.3751	10.1214
Laminin subunit beta-1	ECM Structural component.	Cell migration. Basement membrane assembly	0.3758	2.4942
Sulfhydryl oxidase 1	Flavin-linked sulfhydryl oxidase activity	Cellular protein metabolic process. ECM assembly	0.3939	9.0644
Tropomyosin alpha-4 chain	Actin filament binding	actin filament organization	0.4428	1.6735
Cathepsin L1	Cysteine-type endopeptidase activity	Collagen catabolic process	0.4633	1.9447
Collagen alpha-1(V) chain	ECM Structural component. Heparin binding	Collagen biosynthetic process and organization. Cell migration and adhesion	0.4680	3.6270
Nucleoside diphosphate kinase	Deoxyribonuclease activity	Differentiation. Endocytosis. Neurogenesis. Nucleotide metabolism	0.4680	1.9268
Cathepsin Z	Cysteine-type endopeptidase activity	Proteolysis. Endoplasmic reticulum to Golgi vesicle-mediated transport	0.4773	1.6631
Glia-derived nexin	Serine-type endopeptidase inhibitor activity	Innervation. Inhibiting thrombin	0.4817	6.2818

Journal Pre-proof

Journal Pre-proof

Table S2. "GOTERM" List

EXTRACELLULAR MATRIX			
GO TERM	**NUMBER**	**GO TERM**	**NUMBER**
regulation of cell-matrix adhesion	GO:0001952	extracellular matrix constituent secretion	GO:0070278
negative regulation of cell-matrix adhesion	GO:0001953	cellular response to cell-matrix adhesion	GO:0071460
positive regulation of cell-matrix adhesion	GO:0001954	extracellular matrix assembly	GO:0085029
regulation of extracellular matrix constituent secretion	GO:0003330	positive regulation of extracellular matrix disassembly	GO:0090091
positive regulation of extracellular matrix constituent secretion	GO:0003331	endothelial cell-matrix adhesion	GO:0090673
negative regulation of extracellular matrix constituent secretion	GO:0003332	endothelial cell-matrix adhesion via fibronectin	GO:0090674
cell-matrix adhesion involved in mesendodermal cell migration	GO:0003368	cell-matrix adhesion mediator activity	GO:0098634
extracellular matrix structural constituent	GO:0005201	protein complex involved in cell-matrix adhesion	GO:0098637
cell-matrix adhesion	GO:0007160	laminin binding involved in cell-matrix adhesion	GO:0098638
calcium-independent cell-matrix adhesion	GO:0007161	collagen binding involved in cell-matrix adhesion	GO:0098639
regulation of extracellular matrix disassembly	GO:0010715	integrin binding involved in cell-matrix adhesion	GO:0098640
negative regulation of extracellular matrix disassembly	GO:0010716	synaptic membrane adhesion to extracellular matrix	GO:0099561
calcium-dependent cell-matrix adhesion	GO:0016340	gene expression involved in extracellular matrix organization	GO:1901148
extracellular matrix disassembly	GO:0022617	regulation of extracellular matrix assembly	GO:1901201
extracellular matrix structural constituent conferring tensile strength	GO:0030020	negative regulation of extracellular matrix assembly	GO:1901202
extracellular matrix structural constituent conferring compression resistance	GO:0030021	positive regulation of extracellular matrix assembly	GO:1901203
extracellular matrix organization	GO:0030198	regulation of extracellular matrix organization	GO:1903053
extracellular matrix	GO:0031012	negative regulation of extracellular matrix organization	GO:1903054
extracellular matrix-cell signaling	GO:0035426	positive regulation of extracellular matrix organization	GO:1903055
sequestering of BMP in extracellular matrix	GO:0035582	regulation of collagen fibril organization	GO:1904026
sequestering of TGFbeta in extracellular matrix	GO:0035583	regulation of endothelial cell-matrix adhesion via fibronectin	GO:1904904
extracellular matrix component	GO:0044420	negative regulation of endothelial cell-matrix adhesion via fibronectin	GO:1904905
extracellular matrix binding	GO:0050840	positive regulation of endothelial cell-matrix adhesion via fibronectin	GO:1904906
smooth muscle cell-matrix adhesion	GO:0061302	positive regulation of smooth muscle cell-matrix adhesion	GO:1905609
collagen-containing extracellular matrix	GO:0062023	extracellular matrix protein binding	GO:1990430
negative regulation of smooth muscle cell-matrix adhesion	GO:2000098	regulation of smooth muscle cell-matrix adhesion	GO:2000097
MIGRATION			
GO TERM	**NUMBER**	**GO TERM**	**NUMBER**
epidermal growth factor receptor signaling pathway	GO:0007173	wound healing, spreading cells	GO:0044319
negative regulation of epidermal growth factor-activated receptor activity	GO:0007175	negative regulation of cell migration in other organism	GO:0044622
regulation of epidermal growth factor-activated receptor activity	GO:0007176	positive regulation of cell migration in other organism	GO:0044623
epithelial cell migration	GO:0010631	positive regulation of epidermal growth factor-activated receptor activity	GO:0045741
regulation of epithelial cell migration	GO:0010632	positive regulation of epidermal growth factor receptor signaling pathway	GO:0045742
negative regulation of epithelial cell migration	GO:0010633	keratinocyte migration	GO:0051546
positive regulation of epithelial cell migration	GO:0010634	regulation of keratinocyte migration	GO:0051547
fibroblast migration	GO:0010761	negative regulation of keratinocyte migration	GO:0051548
regulation of fibroblast migration	GO:0010762	positive regulation of keratinocyte migration	GO:0051549
positive regulation of fibroblast migration	GO:0010763	epithelium migration	GO:0090132
negative regulation of fibroblast migration	GO:0010764	epithelial cell-cell adhesion involved in epithelium migration	GO:0090137
cell migration	GO:0016477	regulation of epithelial cell-cell adhesion involved in epithelium migration	GO:1903681
regulation of cell migration	GO:0030334	negative regulation of epithelial cell-cell adhesion involved in epithelium migration	GO:1903682
positive regulation of cell migration	GO:0030335	positive regulation of epithelial cell-cell adhesion involved in epithelium migration	GO:1903683
negative regulation of cell migration	GO:0030336	regulation of wound healing spreading of epidermal cells	GO:1903689
regulation of epidermal growth factor receptor signaling pathway	GO:0042058	negative regulation of wound healing, spreading of epidermal cells	GO:1903690
negative regulation of epidermal growth factor receptor signaling pathway	GO:0042059	positive regulation of wound healing, spreading of epidermal cells	GO:1903691
Rho GDP-dissociation inhibitor activity	GO:0005094		
ANGIOGENESIS			
GO TERM	**NUMBER**	**GO TERM**	**NUMBER**
angiogenesis	GO:0001525	positive regulation of cell adhesion involved in sprouting angiogenesis	GO:0106090
endothelial cell proliferation	GO:0001935	positive regulation of blood vessel endothelial cell differentiation	GO:0110058
regulation of endothelial cell proliferation	GO:0001936	negative regulation of blood vessel endothelial cell differentiation	GO:0110059
negative regulation of endothelial cell proliferation	GO:0001937	cell adhesion involved in sprouting angiogenesis	GO:0120078
positive regulation of endothelial cell proliferation	GO:0001938	positive regulation of vascular endothelial growth factor signaling pathway	GO:1900748
sprouting angiogenesis	GO:0002040	negative regulation of endothelial cell development	GO:1901551
cell migration involved in sprouting angiogenesis	GO:0002042	positive regulation of endothelial cell development	GO:1901552
regulation of cell adhesion involved in intussusceptive angiogenesis	GO:0002045	negative regulation of establishment of endothelial barrier	GO:1903141
positive regulation of vascular endothelial growth factor production	GO:0010575	positive regulation of establishment of endothelial barrier	GO:1903142
positive regulation of endothelial cell migration	GO:0010595	negative regulation of blood vessel endothelial cell proliferation involved in sprouting angiogenesis	GO:1903588
negative regulation of endothelial cell migration	GO:0010596	positive regulation of blood vessel endothelial cell proliferation involved in sprouting angiogenesis	GO:1903589
negative regulation of angiogenesis	GO:0016525	regulation of sprouting angiogenesis	GO:1903670
positive regulation of vascular endothelial growth factor receptor signaling pathway	GO:0030949	negative regulation of sprouting angiogenesis	GO:1903671
positive regulation of blood vessel endothelial cell migration	GO:0043536	positive regulation of sprouting angiogenesis	GO:1903672
negative regulation of blood vessel endothelial cell migration	GO:0043537	negative regulation of endothelial cell activation	GO:1904988
negative regulation of endothelial cell differentiation	GO:0045602	positive regulation of endothelial cell activation	GO:1904989
positive regulation of endothelial cell differentiation	GO:0045603	negative regulation of endothelial tube morphogenesis	GO:1905955
regulation of angiogenesis	GO:0045765	positive regulation of endothelial tube morphogenesis	GO:1905956
positive regulation of angiogenesis	GO:0045766	positive regulation of endothelial cell apoptotic process	GO:2000353
angiogenesis involved in wound healing	GO:0060055	negative regulation of venous endothelial cell fate commitment	GO:2000788
angiogenesis involved in coronary vascular morphogenesis	GO:0060978	positive regulation of venous endothelial cell fate commitment	GO:2000789
cell migration involved in coronary angiogenesis	GO:0060981	negative regulation of endothelial cell chemotaxis	GO:2001027
regulation of cell migration involved in sprouting angiogenesi	GO:0090049	vascular endothelial cell proliferation	GO:0101023
positive regulation of cell migration involved in sprouting angiogenesis	GO:0090050	regulation of cell adhesion involved in sprouting angiogenesis	GO:0106088
negative regulation of cell migration involved in sprouting angiogenesis	GO:0090051		
EPIDERMAL DIFFERENTIATION			
GO TERM	**NUMBER**	**GO TERM**	**NUMBER**
positive regulation of keratinocyte differentiation	GO:0045618	regulation of epidermal cell differentiation	GO:0045604
positive regulation of cell differentiation	GO:0045597	regulation of epidermal cell division	GO:0010482
positive regulation of epidermal cell differentiation	GO:0045606	keratinocyte differentiation	GO:0030216
negative regulation of keratinocyte differentiation	GO:0045617	regulation of cell maturation	GO:1903429
negative regulation of cell differentiation	GO:0045596	epidermal cell differentiation	GO:0009913
negative regulation of epidermal cell differentiation	GO:0045605	regulation of epidermal cell differentiation	GO:0045604
regulation of keratinocyte differentiation	GO:0045616	epithelial cell differentiation	GO:0030855
epidermal cell differentiation	GO:0009913	polarized epithelial cell differentiation	GO:0030859

Journal Pre-proof

ECM REMODELING			
GO TERM	**NUMBER**	**GO TERM**	**NUMBER**
clearance of damaged tissue involved in inflammatory response wound healing	GO:0002247	regulation of connective tissue replacement	GO:1905203
connective tissue replacement involved in inflammatory response wound healing	GO:0002248	negative regulation of connective tissue replacement	GO:1905204
regulation of tissue remodeling	GO:0034103	positive regulation of connective tissue replacement	GO:1905205
negative regulation of tissue remodeling	GO:0034104	regulation of blood vessel remodeling	GO:0060312
positive regulation of tissue remodeling	GO:0034105	negative regulation of blood vessel remodeling	GO:0060313
tissue regeneration	GO:0042246	blood vessel remodeling	GO:0001974
tissue remodeling	GO:0048771	positive regulation of blood vessel remodeling	GO:2000504
connective tissue development	GO:0061448	protein-containing complex remodeling	GO:0034367
connective tissue replacement	GO:0097709	TIMP family protein binding	GO:0098769
regulation of connective tissue replacement involved in inflammatory response wound healing	GO:1904596	positive regulation of matrix metallopeptidase secretion	GO:1904466
negative regulation of connective tissue replacement involved in inflammatory response wound healing	GO:1904597	negative regulation of matrix metallopeptidase secretion	GO:1904465
positive regulation of connective tissue replacement involved in inflammatory response wound healing	GO:1904598	regulation of matrix metallopeptidase secretion	GO:1904464
matrix metallopeptidase secretion	GO:1990773		
PROLIFERATION			
GO TERM	**NUMBER**	**GO TERM**	**NUMBER**
cell proliferation	GO:0008283	positive regulation of epithelial cell proliferation	GO:0050679
positive regulation of cell proliferation	GO:0008284	negative regulation of epithelial cell proliferation	GO:0050680
negative regulation of cell proliferation	GO:0008285	positive regulation of epithelial cell proliferation involved in wound healing	GO:0060054
mesenchymal cell proliferation	GO:0010463	regulation of stem cell proliferation	GO:0072091
regulation of mesenchymal cell proliferation	GO:0010464	condensed mesenchymal cell proliferation	GO:0072137
regulation of keratinocyte proliferation	GO:0010837	negative regulation of mesenchymal cell proliferation	GO:0072201
negative regulation of keratinocyte proliferation	GO:0010839	mesenchymal stem cell proliferation	GO:0097168
positive regulation of keratinocyte proliferation	GO:0010838	regulation of mesenchymal stem cell proliferation	GO:1902460
regulation of cell proliferation	GO:0042127	negative regulation of mesenchymal stem cell proliferation	GO:1902461
keratinocyte proliferation	GO:0043616	positive regulation of mesenchymal stem cell proliferation	GO:1902462
fibroblast proliferation	GO:0048144	negative regulation of stem cell proliferation	GO:2000647
regulation of fibroblast proliferation	GO:0048145	positive regulation of stem cell proliferation	GO:2000648
positive regulation of fibroblast proliferation	GO:0048146	Rho GDP-dissociation inhibitor activity	GO:0005094
negative regulation of fibroblast proliferation	GO:0048147	mitotic DNA replication termination	GO:1902979
epithelial cell proliferation	GO:0050673	phosphatidylinositol-3-phosphate biosynthetic process	GO:0036092
regulation of epithelial cell proliferation	GO:0050678	1-phosphatidylinositol-3-kinase activity	GO:0016303
WOUND			
GO TERM	**NUMBER**	**GO TERM**	**NUMBER**
positive regulation of wound healing	GO:0090303	angiogenesis involved in wound healing	GO:0060055
inflammatory response to wounding	GO:0090594	positive regulation of epithelial cell proliferation involved in wound healing	GO:0060054
negative regulation of wound healing	GO:0061045	positive regulation of inflammatory response to wounding	GO:0106016
regulation of wound healing	GO:0061041	negative regulation of inflammatory response to wounding	GO:0106015
vascular wound healing	GO:0061042	regulation of inflammatory response to wounding	GO:0106014
regulation of vascular wound healing	GO:0061043	Wnt signaling pathway involved in wound healing, spreading of epidermal cells	GO:0035659
negative regulation of vascular wound healing	GO:0061044	positive regulation of vascular wound healing	GO:0035470
wound healing involved in inflammatory response	GO:0002246	wound healing	GO:0042060
clearance of damaged tissue involved in inflammatory response wound healing	GO:0002247	positive regulation of connective tissue replacement involved in inflammatory response wound healing	GO:1904598
connective tissue replacement involved in inflammatory response wound healing	GO:0002248	negative regulation of connective tissue replacement involved in inflammatory response wound healing	GO:1904597
positive regulation of response to wounding	GO:1903036	regulation of connective tissue replacement involved in inflammatory response wound healing	GO:1904596
regulation of response to wounding	GO:1903034	detection of wounding	GO:0014822
negative regulation of response to wounding	GO:1903035	response to wounding	GO:0009611
behavioral response to wounding	GO:0002210	wound healing, spreading of cells	GO:0044319
regulation of wound healing, spreading of epidermal cells	GO:1903689	canonical Wnt signaling pathway involved in positive regulation of wound healing	GO:0044330
negative regulation of wound healing, spreading of epidermal cells	GO:1903690	Rho GDP-dissociation inhibitor activity	GO:0005094
positive regulation of wound healing, spreading of epidermal cells	GO:1903691	wound healing, spreading of epidermal cells	GO:0035313
AKT SIGNALING			
GO TERM	**NUMBER**	**GO TERM**	**NUMBER**
positive regulation of phosphatidylinositol 3-kinase signaling	GO:0014068	negative regulation of kinase activity	GO:0033673
positive regulation of phosphatidylinositol 3-kinase activity	GO:0043552	regulation of phosphatidylinositol 3-kinase signaling	GO:0014066
positive regulation of 1-phosphatidylinositol-3-kinase activity	GO:0061903	phosphatidylinositol 3-kinase signaling	GO:0014065
positive regulation of 1-phosphatidylinositol-4-phosphate 5-kinase activity	GO:0090216	protein kinase B binding	GO:0043422
positive regulation of phosphatidylinositol-4,5-bisphosphate 5-phosphatase activity	GO:0120139	protein kinase B signaling	GO:0043491
positive regulation of phosphatidylinositol-3,4,5-trisphosphate 5-phosphatase activity	GO:2001146	regulation of protein kinase B signaling	GO:0051896
positive regulation of kinase activity	GO:0033674	positive regulation of protein kinase B signaling	GO:0051897
negative regulation of phosphatidylinositol 3-kinase signaling	GO:0014067	negative regulation of protein kinase B signaling	GO:0051898
negative regulation of phosphatidylinositol 3-kinase activity	GO:0043553	phosphatidylinositol phosphate 5-phosphatase activity	GO:0034595
negative regulation of 1-phosphatidylinositol-3-kinase activity	GO:0061902	phosphatidylinositol phosphate kinase activity	GO:0016307
negative regulation of 1-phosphatidylinositol-4-phosphate 5-kinase activity	GO:0090217	activation of protein kinase B activity	GO:0032148
negative regulation of phosphatidylinositol-4,5-bisphosphate 5-phosphatase activity	GO:0120140	phosphatidylinositol-3-phosphate biosynthetic process	GO:0036092
negative regulation of phosphatidylinositol-3,4,5-trisphosphate 5-phosphatase activity	GO:2001145	1-phosphatidylinositol-3-kinase activity	GO:0016303
SMAD SIGNALING			
GO TERM	**NUMBER**	**GO TERM**	**NUMBER**
positive regulation of pathway-restricted SMAD protein phosphorylation	GO:0010862	negative regulation of pathway-restricted SMAD protein phosphorylation	GO:0060394
negative regulation of SMAD protein complex assembly	GO:0010991	SMAD protein signal transduction	GO:0060395
positive regulation of transforming growth factor beta receptor signaling pathway	GO:0030511	negative regulation of transforming growth factor beta production	GO:0071635
negative regulation of transforming growth factor beta receptor signaling pathway	GO:0030512	positive regulation of transforming growth factor beta production	GO:0071636
regulation of SMAD protein signal transduction	GO:0060390	negative regulation of transforming growth factor beta receptor signaling pathway involved in primitive streak formation	GO:0090012
positive regulation of SMAD protein signal transduction	GO:0060391	negative regulation of transforming growth factor beta activation	GO:1901389
negative regulation of SMAD protein signal transduction	GO:0060392	positive regulation of transforming growth factor beta activation	GO:1901390
regulation of pathway-restricted SMAD protein phosphorylation	GO:0060393	positive regulation of transforming growth factor-beta secretion	GO:2001203
MAPK CASCADE			
GO TERM	**NUMBER**	**GO TERM**	**NUMBER**
MAPK cascade	GO:0000165	regulation of MAPK cascade	GO:0043408
activation of MAPKKK activity involved in osmosensory signaling pathway	GO:0000167	negative regulation of MAPK cascade	GO:0043409
activation of MAPKK activity involved in osmosensory signaling pathway	GO:0000168	positive regulation of MAPK cascade	GO:0043410

Journal Pre-proof

activation of MAPK activity involved in osmosensory signaling pathway	GO:0000169	inactivation of MAPKK activity	GO:0051389
inactivation of MAPK activity involved in osmosensory signaling pathway	GO:0000173	inactivation of MAPKKK activity	GO:0051390
activation of MAPKKK activity	GO:0000185	stress activated MAPK cascade	GO:0051403
activation of MAPKK activity	GO:0000186	negative regulation by organism of defense-related MAP kinase-mediated signal transduction pathway in other organism involved in symbiotic interaction	GO:0052275
activation of MAPK activity	GO:0000187	positive regulation by organism of defense-related MAP kinase-mediated signal transduction pathway in other organism involved in symbiotic interaction	GO:0052276
inactivation of MAPK activity	GO:0000188	positive regulation by host of defense-related symbiont MAP kinase-mediated signal transduction pathway	GO:0052502
activation of MAPKKK activity involved in cell wall organization or biogenesis	GO:0000197	positive regulation of pheromone response MAPK cascade	GO:0062038
activation of MAPKK activity involved in cell wall organization or biogenesis	GO:0000198	negative regulation of ERK1 and ERK2 cascade	GO:0070373
activation of MAPK activity involved in cell wall organization or biogenesis	GO:0000199	positive regulation of ERK1 and ERK2 cascade	GO:0070374
inactivation of MAPK activity involved in cell wall organization or biogenesis	GO:0000200	activation of MAPK activity involved in conjugation with cellular fusion	GO:0071508
negative regulation of stress-activated MAPK cascade	GO:0032873	activation of MAPKK activity involved in conjugation with cellular fusion	GO:0071509
positive regulation of stress-activated MAPK cascade	GO:0032874	activation of MAPKKK activity involved in conjugation with cellular fusion	GO:0071510
activation of MAPK activity involved in innate immune response	GO:0035419	inactivation of MAPK activity involved in conjugation with cellular fusion	GO:0071511
activation of MAPK activity involved in innate immune response	GO:0035419	positive regulation of MAPKKK cascade by fibroblast growth factor receptor signaling pathway	GO:0090080
activation of MAPKK activity involved in innate immune response	GO:0035421	positive regulation of p38MAPK cascade	GO:1900745
activation of MAPKKK activity involved in innate immune response	GO:0035422	regulation of MAPK cascade involved in cell wall organization or biogenesis	GO:1903137
inactivation of MAPK activity involved in innate immune response	GO:0035423	negative regulation of MAPK cascade involved in cell wall organization or biogenesis	GO:1903138
epidermal growth factor receptor signaling pathway via MAPK cascade	GO:0038029	negative regulation of MAPK cascade involved in cell wall organization or biogenesis	GO:1903138
MAP kinase activity involved in innate immune response	GO:0038075	positive regulation of MAPK cascade involved in cell wall organization or biogenesis	GO:1903139
regulation of MAP kinase activity	GO:0043405	positive regulation of MAPK cascade involved in cell wall organization or biogenesis	GO:1903139
positive regulation of MAP kinase activity	GO:0043406	negative regulation of MAP kinase activity	GO:0043407
INTEGRIN SIGNALING			
GO TERM	**NUMBER**	**GO TERM**	**NUMBER**
integrin-mediated signaling pathway	GO:0007229	negative regulation of cell adhesion mediated by integrin	GO:0033629
regulation of integrin-mediated signaling pathway	GO:2001044	regulation of cell adhesion mediated by integrin	GO:0033628
negative regulation of integrin-mediated signaling pathway	GO:2001045	cell adhesion mediated by integrin	GO:0033627
positive regulation of integrin-mediated signaling pathway	GO:2001046	positive regulation of integrin activation by cell surface receptor linked signal transduction	GO:0033626
regulation of integrin biosynthetic process	GO:0045113	positive regulation of integrin activation	GO:0033625
integrin complex	GO:0008305	negative regulation of integrin activation	GO:0033624
integrin binding involved in cell-matrix adhesion	GO:0098640	regulation of integrin activation	GO:0033623
integrin binding	GO:0005178	integrin activation	GO:0033622
regulation of cell-cell adhesion mediated by integrin	GO:0033632	regulation of integrin-mediated signaling pathway	GO:2001044
cell-cell adhesion mediated by integrin	GO:0033631	negative regulation of integrin-mediated signaling pathway	GO:2001045
positive regulation of cell adhesion mediated by integrin	GO:0033630	positive regulation of integrin-mediated signaling pathway	GO:2001046
positive regulation of cell-cell adhesion mediated by integrin	GO:0033634	integrin-mediated signaling pathway	GO:0007229
negative regulation of cell-cell adhesion mediated by integrin	GO:0033633		
Wnt Signaling			
GO TERM	**NUMBER**		
positive regulation of Wnt signaling pathway by BMP signaling pathway	GO:0060804	positive regulation of Wnt-Frizzled-LRP5/6 complex assembly	GO:1904712
regulation of canonical Wnt signaling pathway	GO:0060828	regulation of Wnt-Frizzled-LRP5/6 complex assembly	GO:1904711
receptor internalization involved in canonical Wnt signaling pathway	GO:2000286	negative regulation of Wnt-Frizzled-LRP5/6 complex assembly	GO:1904723
Wnt signaling pathway, regulating spindle positioning	GO:0060069	coreceptor activity involved in Wnt signaling pathway, planar cell polarity pathway	GO:1904929
canonical Wnt signaling pathway	GO:0060070	coreceptor activity involved in canonical Wnt signaling pathway	GO:1904928
Wnt signaling pathway, planar cell polarity pathway	GO:0060071	Wnt signalosome	GO:1990909
positive regulation of Wnt signaling pathway by establishment of Wnt protein localization to extracellular region	GO:0035593	Wnt signaling pathway	GO:0016055
non-canonical Wnt signaling pathway	GO:0035567	negative regulation of canonical Wnt signaling pathway	GO:0090090
Wnt signaling pathway involved in wound healing, spreading of epidermal cells	GO:0035659	Wnt signaling pathway, calcium modulating pathway	GO:0007223
regulation of non-canonical Wnt signaling pathway	GO:2000050	Wnt signaling pathway involved in kidney development	GO:0061289
positive regulation of non-canonical Wnt signaling pathway	GO:2000052	Wnt-Frizzled-LRP5/6 complex	GO:1990851
negative regulation of non-canonical Wnt signaling pathway	GO:2000051	Wnt protein secretion	GO:0061355
positive regulation of Wnt signaling pathway, planar cell polarity pathway	GO:2000096	regulation of Wnt protein secretion	GO:0061356
regulation of Wnt signaling pathway, planar cell polarity pathway	GO:2000095	positive regulation of Wnt protein secretion	GO:0061357
negative regulation of non-canonical Wnt signaling pathway via JNK cascade	GO:1901230	negative regulation of Wnt protein secretion	GO:0061358
regulation of Wnt signaling pathway	GO:0030111	regulation of Wnt signaling pathway by Wnt protein secretion	GO:0061359
negative regulation of Wnt signaling pathway	GO:0030178	Wnt signalosome assembly	GO:1904887
positive regulation of Wnt signaling pathway	GO:0030177	coreceptor activity involved in Wnt signaling pathway	GO:0071936
negative regulation of heart induction by canonical Wnt signaling pathway	GO:0003136	canonical Wnt signaling pathway involved in positive regulation of cell-cell adhesion	GO:0044329
Wnt-activated receptor activity	GO:0042813	canonical Wnt signaling pathway involved in positive regulation of endothelial cell migration	GO:0044328
Wnt-protein binding	GO:0017147	canonical Wnt signaling pathway involved in positive regulation of wound healing	GO:0044330
regulation of Wnt signaling pathway, calcium modulating pathway	GO:0008591	canonical Wnt signaling pathway involved in positive regulation of epithelial to mesenchymal transition	GO:0044334
cell-cell signaling by wnt	GO:0198738	canonical Wnt signaling pathway involved in positive regulation of apoptotic process	GO:0044337
Wnt-Frizzled-LRP5/6 complex assembly	GO:1904701	canonical Wnt signaling pathway involved in negative regulation of apoptotic process	GO:0044336
canonical Wnt signaling pathway involved in stem cell proliferation	GO:1905474	canonical Wnt signaling pathway involved in mesenchymal stem cell differentiation	GO:0044338
non-canonical Wnt signaling pathway via JNK cascade	GO:0038031	canonical Wnt signaling pathway involved in regulation of cell proliferation	GO:0044340
beta-catenin destruction complex disassembly	GO:1904886		

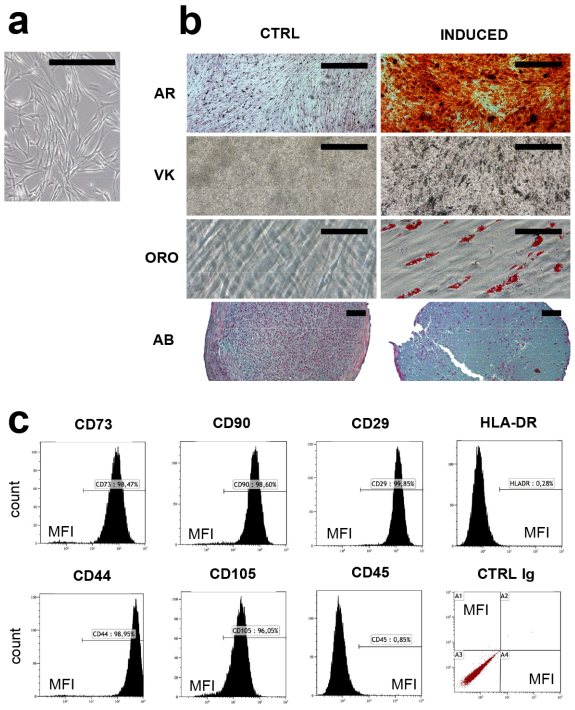

Figure S1. Gingival MSC characterization

Representative pictures of (a) phase-contrast image of plastic-adherent gingival MSCs (scale bar = 200 µm) and of (b) osteogenic, adipogenic and chondrogenic inductions of gingival MSCs (scale bar = 500 µm). (c) Phenotype of gingival MSCs assessed by flow cytometry. AB, Alcian blue; AR, Alizarine Red; CTRL, control, MFI, Mean fluorescence intensity; MSC, mesenchymal stromal cells; ORO, Oil Red O; VK, Von Kossa.

Journal Pre-proof

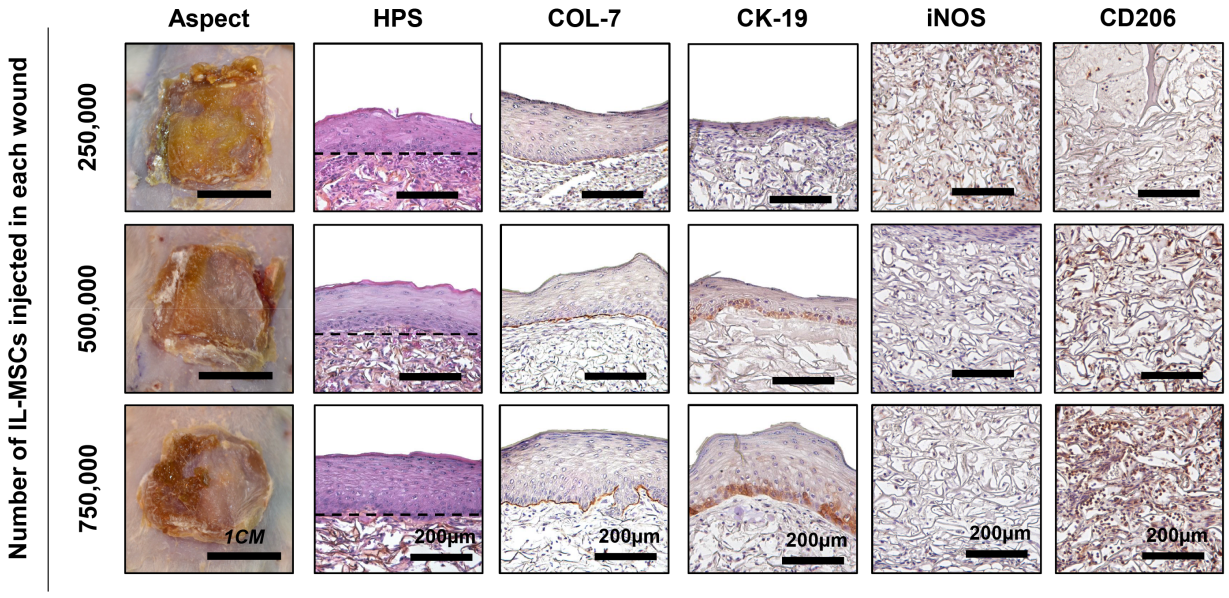

Figure S2. Dose-effect study of IL-MSCs *in vivo.*

IL-MSCs were injected at different doses in NOD/SCID mice treated with Integra and hPBES after full-thickness excisional skin injury (n=6 in each experimental group). Aspect and histology of the skin were observed 14 days after treatment. HPS, Hematoxylin-Phloxin-Safran; COL-7, Collagen-7; CK-19, Cytokeratin-19.

Journal Pre-proof

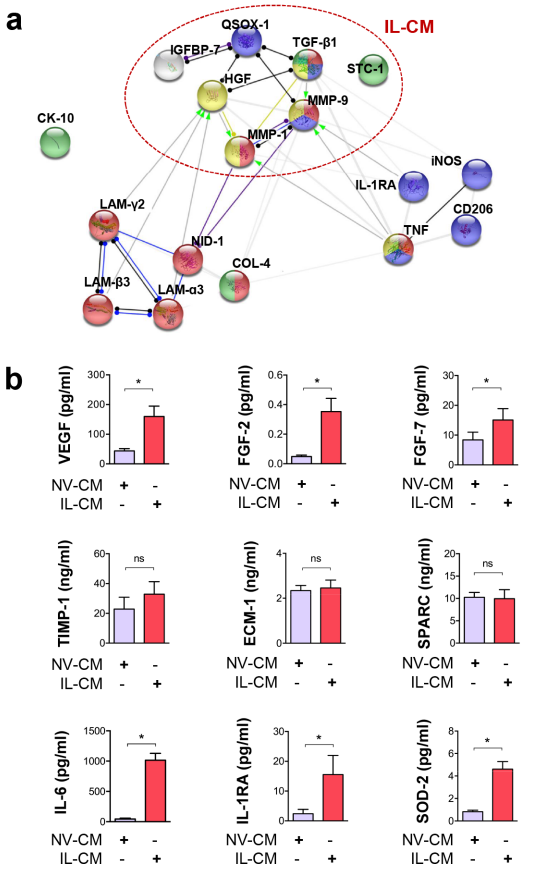

Figure S3. Secretome analysis of naive and IL-1β-primed MSCs

(a) Protein network interaction analysis between selected IL-CM-derived factors and target proteins using the String online database (http://string-db.org/). Proteins in green are correlated with epithelial cell differentiation (GO:0030855), in yellow with cell migration (GO:0016477), in red with ECM organization (GO:0030198) and in blue with immune response (GO:0006955). Links indicate different interaction types, including binding (blue), catalysis (violet), transcription regulation (yellow) and reaction (black). (b) ELISA dosages of selected wound healing-related proteins present in NV- and IL-CM (n= 7). * p<0.05; ns, not significant; CM, conditioned medium; IL, IL-1β; MSC, mesenchymal stromal cells; NV, naive.

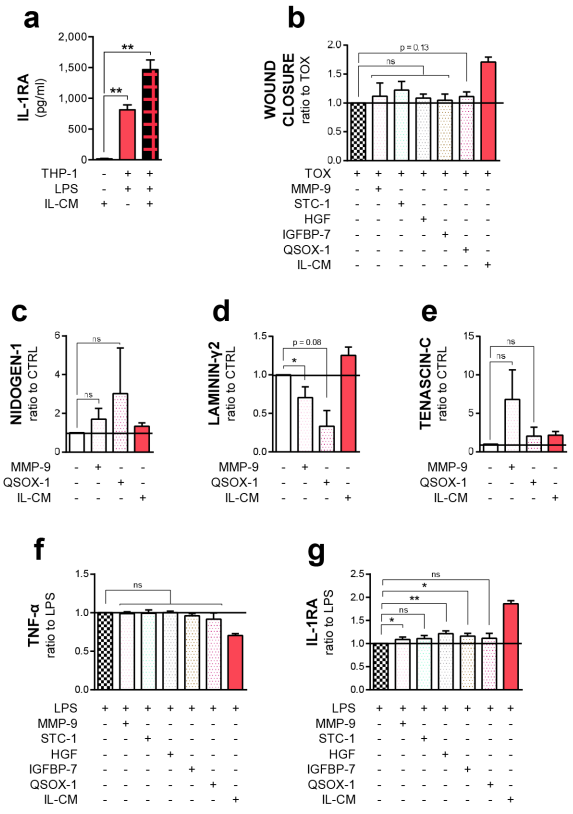

Figure S4. Paracrine mechanisms of action of IL-1β-primed MSCs

(a) Dosage of IL-1RA in IL-CM, and in treated THP-1 culture supernatants (n=7 to 16). (b) Wound closure of intoxicated keratinocytes (TOX) cultured with IL-CM-derived factors (ratio to TOX, n=3 to 7). (c, d, e) Nidogen-1, Tenascin-C and Laminin-γ2 protein expression at 8 days in keratinocyte and fibroblast co-cultures grown with IL-CM-derived factors (ratio to control, n=2 to 5). (f, g) Dosage of TNF-α and IL-1RA in the supernatants of LPS-challenged THP-1 cultured for 24h with IL-CM-derived factors (ratio to LPS control, n=3 to 10). Values are expressed as means± SEM. *p<0.05; **p<0.01; ***p<0.001; ns, not significant. CM, conditioned medium; CTRL, control; IL, IL-1β; LAM-γ2, Laminin-5 γ2 chain; NID-1,Nidogen-1; NV, naive; TNC, Tenascin-C; TOX, intoxicated keratinocytes.

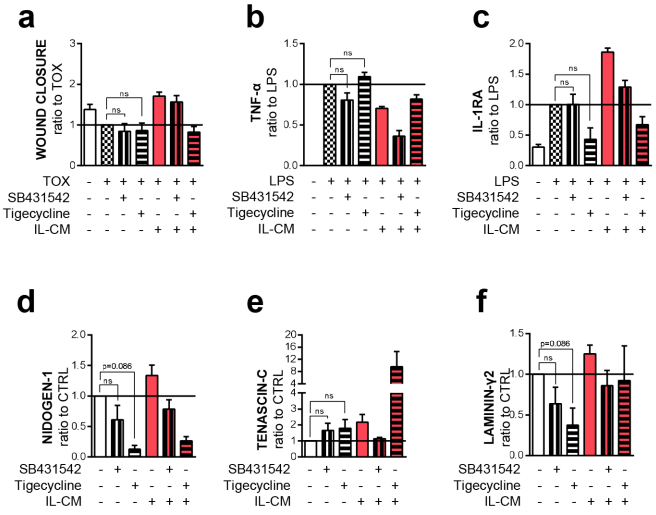

Figure S5. Inhibitors effect on migration, Inflammation and JDE model

(a) Wound closure of intoxicated keratinocytes (TOX) cultured with or without SB431542- or Tigecycline and supplemented or not with IL-CM (ratio to TOX, n=5 to 7). (b) Dosage of TNF-α and (c) of IL-1RA in the supernatants of LPS-challenged THP-1 cultured for 24h with or without SB431542- or Tigecycline and supplemented or not with IL-CM (ratio to LPS control, n=3 to 19). (d) Nidogen-1, (e) Tenascin-C and (f) Laminin-γ2 protein expression at 8 days in keratinocyte and fibroblast co-cultures grown with or without SB431542- or Tigecycline and supplemented or not with IL-CM (ratio to control, n=4 to 7). Values are expressed as means± SEM. ns, not significant. CM, conditioned medium; CTRL, control; IL, IL-1β; LAM-γ2, Laminin-5 γ2 chain; NID-1,Nidogen-1; NV, naive; TNC, Tenascin-C; TOX, intoxicated keratinocytes.

Journal Pre-proof

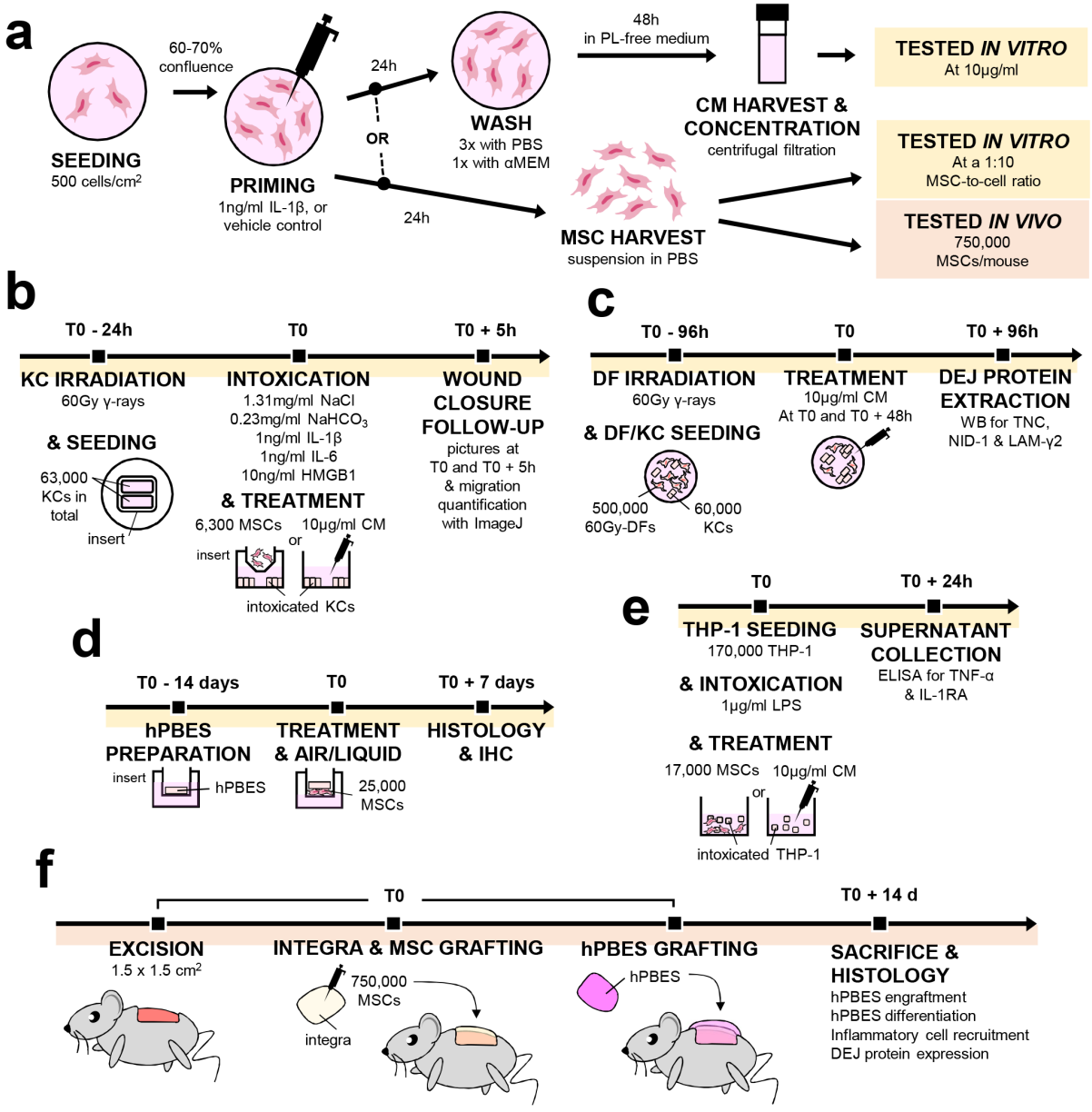

Figure S6. Experimental procedures and assays.

(a) MSC priming and CM preparation procedures. (b) Wound closure assay. (c) DEJ formation assay. (d) Air/liquid epidermal differentiation assay. (e) Inflammation assay. (f) *In vivo* model of dorsal acute wound and hPBES grafting. CM, Conditioned Medium; DEJ, dermal-epidermal junction; DF, dermal fibroblast; hPBES, human plasma-based epidermal substitute; KC, keratinocyte; MSC, mesenchymal stromal cells; PL, platelet lysate.

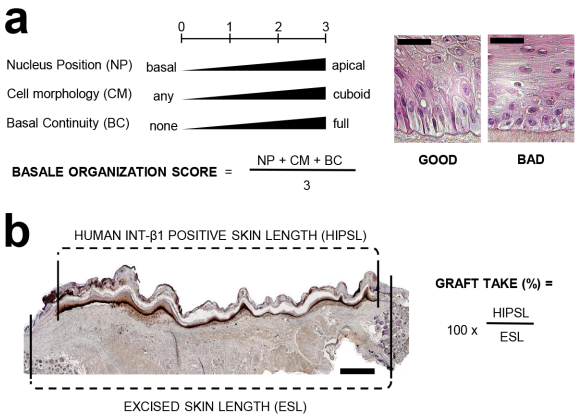

Figure S7. Histological quantifications and scores methods

(a) Method of epidermal basal layer scoring, made by three independent observers, on the basis of nucleus position, cell morphology and basal continuity (scale bar = 50 µm). (b) Method of quantification of hPBES engraftment, based on human Integrin-β1 immunostaining (scale bar = 1500 µm). INT-β1, Integrin-β1; hPBES, human plasma-based epidermal substitute.

Journal Pre-proof